THE DROUGHT RESPONSE OF PHYSIOLOGICAL AND STRUCTURAL TRAITS IN LOBLOLLY PINE (*P. TAEDA* L.) CLONES WITH A FOCUS ON MESOPHYLL CONDUCTANCE TO CO_2

A Thesis

by

ELIZABETH SUSAN WILSON

Submitted to the Office of Graduate and Professional Studies of
Texas A&M University
in partial fulfillment of the requirements for the degree of

MASTER OF SCIENCE

Chair of Committee,	Jason B. West
Co-Chair of Committee,	Jason G. Vogel
Committee Member,	Astrid Volder
Head of Department,	David D. Baltensperger

August 2014

Major Subject: Ecosystem Science and Management

ABSTRACT

Climate change will likely affect the productivity of forests through changes in precipitation and moisture availability. An important measure of a plant's ability to assimilate carbon in photosynthesis with limited water loss, water use efficiency (WUE), is assessed by carbon stable isotopes using the Farquhar model. However, recent work has shown that mesophyll conductance to CO_2 (g_m) is affected by environmental conditions, and the simplified model does not take into account this variability. Variation in this parameter could decrease the effectiveness of the stable isotope tool.

A coupled gas exchange and carbon isotope system was developed and tested on well-watered loblolly pine seedlings. A cavity ring-down spectroscopy (CRDS) laser connected to a LI-6400XT gas exchange system allowed simultaneous measurements of photosynthesis and instantaneous carbon isotope discrimination. The standard deviation of two minute averaged delta over ten minute intervals ranged from 0.31‰ to 0.51‰. Mesophyll conductance measured by this system on well-watered loblolly pine seedlings ranged from -0.74 to 0.99 mol m^{-2} s^{-1} and averaged 0.07 ± 0.04 mol m^{-2} s^{-1}.

A greenhouse study was conducted of the drought effects on g_m and other physical and biochemical traits in three clones of loblolly pine (*P. taeda* L.). Stomatal and hydraulic sensitivity to drought was assessed in the clones. Mesophyll conductance was estimated using several methods: gas exchange curve fitting, the variable J method of chlorophyll fluorescence, carbon isotope discrimination from leaf soluble

carbohydrates, and instantaneous carbon isotope discrimination using a cavity ring-down spectroscopy laser.

The three clones exhibited plasticity in stomatal conductivity and hydraulic conductivity in response to drought. The fastest growing clone also had the highest hydraulic conductivity and lowest WUE in well-watered conditions. There were no significant clonal or drought effects on g_m, suggesting that the simplified Farquhar model is adequate for the use of stable isotopes as a proxy for WUE.

ACKNOWLEDGMENTS

I would like to thank my committee co-chairs, Dr. Jason West and Dr. Jason Vogel, and my committee member, Dr. Astrid Volder, for their guidance and involvement throughout the course of this research.

I would also like to thank JC Domec and his lab at Duke University for hydraulic conductance measurements. Thank you to the people who helped in this research: my parents, Rick and Jane Wilson, undergraduate research intern, Madison Wigley, lab managers, Ayumi Hyodo and Tim Rogers, Tom Byram and David Dickinson of the Forestry Service, and the members of the West and Vogel lab groups.

This research was part of the Pine Integrated Network: Education, Mitigation, and Adaptation project (PINEMAP), a Coordinated Agricultural Project funded by the USDA National Institute of Food and Agriculture, Award #2011-68002-30185.

NOMENCLATURE

A_n	Net photosynthesis
C_a	Ambient CO_2 concentration
C_c	Chloroplast CO_2 concentration
C_i	Internal CO_2 concentration
CRDS	Cavity ring-down spectroscopy
$\delta^{13}C_{bl}$	Standardized carbon-13 composition of bulk leaf
$\delta^{13}C_{sam}$	Standardized carbon-13 composition of sample gas
$\delta^{13}C_{sc}$	Standardized carbon-13 composition of leaf soluble carbohydrates
$\delta^{13}C_{ref}$	Standardized carbon-13 composition of reference gas
Γ^*	Chloroplastic photocompensation point
g_m	Mesophyll conductance
g_s	Stomatal conductance
J	Electron transport rate
K_s	Stem conductivity
LMA	Leaf mass per unit area
LSC	Leaf specific conductivity
P_{50}	Pressure at 50% conductance loss
R_d	Day respiration without photorespiration
RGR	Relative rate of change in biomass
SLA	Specific leaf area

WUE	Water use efficiency
WUE_i	Intrinsic water use efficiency, A/g_s
Ψ_{PD}	Pre-dawn water potential
Ψ_{MD}	Mid-day water potential

TABLE OF CONTENTS

Page

LIST OF FIGURES

Page

Page

LIST OF TABLES

Page

INTRODUCTION

Climate change will likely affect the productivity of forests through changes in precipitation and moisture availability. Some regions may experience more severe droughts caused by an increase in greenhouse gases in the atmosphere (Stocker 2013). Drought stress can decrease growth and affect the reproduction of plants (Jones 1992), and drought is associated with many recent occurrences of forest mortality (Allen et al. 2010). On a larger scale, drought decreases regional net primary productivity, which decreases carbon sequestration (Zhao and Running 2010). The ability of trees to assimilate carbon by photosynthesis while transpiring less water (water use efficiency, WUE) and to avoid or tolerate drought stress is important for their survival and growth.

Plants adapt to tolerate or avoid drought conditions in several ways. Drought tolerance is a plant's ability to maintain functionality while experiencing water stress. In contrast, some plants avoid drought by entering dormancy in low water conditions or by preventing low water potentials. This includes leaf morphology that reduces water loss, high stomatal sensitivity, or deep taproots for accessing water (Kramer 1983, Jones 1992, Kozlowski and Pallardy 2002). Deciduous trees may avoid mortality by shedding leaves during drought. Adaptations to drought can limit photosynthesis.

One trait that can respond to drought is hydraulic conductivity. The structure of the hydraulic vessels determines a tree's ability to conduct water to the leaves. Vessel length and pit conductance control hydraulic conductivity (Sperry et al. 2006). Vessel structure that allows faster flow can also make the vessels more vulnerable to cavitation

(Sperry et al. 2006). Cavitation occurs when high tension causes air to enter the vessel, called an embolism, and renders the vessel incapable of conducting water until repaired. Cavitation may occur at high or low water potentials depending on the vessel structure. The vulnerability to cavitation is affected by vessel structure, indirectly by conduit length and width due to end-wall resistivity, and directly by pit pore area in xylem, pit structure in tracheids, and wood density (Hacke et al. 2006, Sperry et al. 2006, Domec et al. 2010). Wood density is correlated to cell wall thickness, which prevents conduit implosion at high tension, but tracheids must have thick cell walls to provide structural support, and little variation in cell wall thickness is seen in conifers (Pittermann et al. 2006). There is a trade-off between stem conductivity and the vulnerability to cavitation from structural acclimation under water stress (Domec et al. 2010).

Leaf specific conductivity (LSC) measures the stem's ability to supply water to the leaves (Tyree and Ewers 1991). It is calculated from stem conductivity (K_s) multiplied by xylem area divided by total leaf area, which yields the conductivity for a ratio of xylem to leaf area. LSC is strongly and positively correlated to photosynthetic rates in various species (Brodribb et al. 2000). Stomatal conductance and hydraulic conductivity are directly related, and stomatal aperture responds to soil water availability to avoid cavitation at low water potentials (Sperry 2000).

Plants directly control the amount of water transpired from the leaves by the stomatal aperture. Closed stomata reduce transpiration, but as a consequence, less CO_2 enters the leaf for photosynthesis. Stomatal conductance must respond to decreases in

hydraulic conductivity to avoid cavitation levels that cause hydraulic failure (Sperry 2000).

Trees also can respond to drought by changing biomass allocation from leaves and stems to root growth (Jones 1992). An increase in root area relative to leaf area potentially increases the water uptake for a given leaf area. Woody plants generally have a small change in allocation in response to drought (Poorter and Nagel 2000).

This ability of individuals to respond to the environment and a single genotype to display a range of phenotypes is termed plasticity (Sultan 2000). To examine genetic control of a trait, the genotype must be controlled. Plasticity in plants can be most easily studied by comparing clones from asexual propagation.

Global patterns in coordination of leaf traits have been found and collectively termed the "Worldwide Leaf Economic Spectrum" (Wright et al. 2004). A relationship exists between long leaf life-span, high leaf mass per unit area (LMA), low photosynthetic capacity, and low leaf nitrogen content (Wright et al. 2004, Tjoelker et al. 2005, Donovan et al. 2014).

One tool used to determine WUE is stable isotopes. WUE is an important measure of plant water use and carbon assimilation. It is examined at many different scales, and it can be defined at the leaf level as the carbon assimilated in photosynthesis divided by the water transpired. The sources of variation in carbon isotopic composition of plants are known: both the fractionation processes that cause a difference in the isotopic composition between the source air and leaf material and the environmental factors that control the plant isotopic composition (Farquhar et al. 1989). Thus, stable

isotopes are an important tool for studying plant physiological and ecological patterns (Bowling et al. 2008, Marshall et al. 2008).

The longstanding model for all work on carbon isotopes in plants is the Farquhar model (Farquhar et al. 1982). Interpreting this model depends on a relationship between the relative abundance of carbon-13 ($\delta^{13}C$) in the photosynthetic products and the CO_2 concentration in intercellular spaces (C_i). C_i is controlled primarily by stomatal conductance (g_s) and the carboxylation rate in photosynthesis. As g_s decreases, transpiration decreases along with C_i. Assuming constant photosynthesis, a decrease in g_s and C_i will cause a higher $\delta^{13}C$ of plant tissue. Less discrimination against ^{13}C occurs during carboxylation when CO_2 concentration at the site of photosynthesis (C_c) is small and relatively enriched in $\delta^{13}C$ due to the limitation of g_s and the drawdown of CO_2 by photosynthesis. Thus, $\delta^{13}C$ has been used as a proxy for WUE based on control of g_s by plants.

The isotopic composition of plants varies by plant parts, chemical compounds, and time. Leaves are composed of different organic compounds, including carbohydrates, proteins, amino acids, and lipids, that vary in isotopic composition due to fractionations in biochemical processes (Hobbie and Werner 2004). Starches have been shown to be more ^{13}C enriched than soluble carbohydrates (Brugnoli et al. 1988, Göttlicher et al. 2006). Soluble carbohydrates are the most recent C pool. The isotopic composition of phloem sap, which is transported sugars, reflects the past one to two days of g_s (depending on the rate of carbon turnover; Brugnoli et al. 1988, Keitel et al. 2003). Bulk leaf isotopic composition integrates a longer time scale, including C assimilated

during the leaf development or before. The difference in time scale between soluble carbohydrates and bulk leaf tissue affects the use of carbon stable isotopes as a proxy for WUE and for estimating g_m. The discrimination value from soluble carbohydrates ($\delta^{13}C_{sc}$) is much more effective than the discrimination value from bulk leaf tissue ($\delta^{13}C_{bl}$) in predicting C_i/C_a from the Farquhar model (Monti et al. 2006).

Recent work is calling into question the mechanistic basis of the Farquhar model (Evans et al. 1986, Lloyd et al. 1992, Douthe et al. 2011, Tazoe et al. 2011). In their seminal paper, Farquhar et al. (1982) noted the drawdown of CO_2 from the intercellular spaces to the site of carboxylation, saying that the mesophyll conductance of CO_2 (g_m) is finite but large. Thus, the classic Farquhar model assumed infinite g_m and does not include variation in g_m. The problem with eliminating g_m from the model is that g_s controls C_i, but $\delta^{13}C$ is dependent on the CO_2 concentration at the site of photosynthesis (C_c), where C is fixed by ribulose-1,5-bisphosphate carboxylase/ oxygenase (RUBISCO). As a result, if the CO_2 diffusional pathway through the mesophyll varies, the simplified model neglects this variation in relating $\delta^{13}C$ with g_s. The role of g_m in plant function is not well understood but there is increasing evidence that it is an important and variable trait that limits photosynthesis (Warren and Adams 2006).

If g_m is variable, the model needs to account for it in order to relate $\delta^{13}C$ to WUE. Recent observations show that g_m deviates from g_s in some genotypes more than others and is affected by factors such as temperature (Barbour et al. 2010, Evans and Von Caemmerer 2012). Mesophyll conductance has been shown to be less sensitive than g_s to water stress (Bunce 2009) and can recover from drought stress (Centritto et al. 2009,

Flexas et al. 2009). Mesophyll conductance correlates to photosynthetic capacity (von Caemmerer and Evans 1991).

Leaf structure can affect g_m by traits such as mesophyll thickness, chloroplast surface area next to intercellular spaces, and cell wall thickness (Galmés et al. 2013). These traits contribute to the leaf mass per unit area (LMA). A higher LMA or thicker leaf causes a longer path length from intercellular space to the site of carboxylation, which decreases g_m (Gu et al. 2012). The leaf structure may change with leaf age and development and light level (Warren 2005, Tosens et al. 2012). LMA has been seen to increase under drought stress (Ferrio et al. 2009, Gu et al. 2012). In one study, mesophyll conductance tended to increase with increasing mesophyll airspace but did not correlate with mesophyll cell wall area per planar leaf area (Loreto et al. 1992). A leaf-averaged value for g_m is effective even though the path length differs for each RUBISCO molecule, which occupy different positions within the leaf (Sharkey 2012).

Woody plants, and especially conifers, have lower g_m than other plants (Epron et al. 1995, Manter and Kerrigan 2004, Flexas et al. 2008). In a review of estimates of g_m from ninety studies, Flexas et al. (2008) show that evergreen gymnosperms and CAM plants have the lowest g_m (below 0.1 mol m^{-2} s^{-1} bar^{-1}), evergreen and deciduous angiosperms and perennial herbs have moderate g_m (between 0.1 and 0.25 mol m^{-2} s^{-1} bar^{-1}), and herbaceous annuals have the highest g_m (between 0.4 and 0.5 mol m^{-2} s^{-1} bar^{-1}). Some genera or functional groups have wide variability in g_m, while others do not, and the authors suggest that g_m is a rapidly adapting trait (Flexas et al. 2008). A_n of low g_m plants is more sensitive to increasing CO_2 in the atmosphere due to the suppression of

photorespiration (Loreto et al. 1992). In the absence of other limiting factors, rising CO_2 levels could affect the productivity of trees more than that of herbaceous plants.

Understanding g_m is relevant to plant breeding. If genotypes can be selected for g_s and g_m separately, both A and WUE could be increased (Gu et al. 2012, Peguero-Pina et al. 2012). Stomatal conductance and mesophyll conductance have been shown to vary independently (Tazoe et al. 2011). There is evidence for genetic control of g_m and its limitation on maximum photosynthesis in well watered conditions (Gu et al. 2012). Another avenue of breeding for increased photosynthesis is to engineer the leaf anatomy to reduce mesophyll resistance (Tholen et al. 2012). Studies suggest that engineering plants for higher g_m can make a difference in productivity because it can be a major limiting factor in photosynthesis (Peguero-Pina et al. 2012).

DEVELOPMENT OF COUPLED GAS EXCHANGE AND CARBON ISOTOPE DISCRIMINATION SYSTEM

Introduction

Carbon stable isotope discrimination is used as a proxy for WUE by the Farquhar et al. model (1982), but mesophyll conductance was assumed to be fixed and was not included. The difference between the observed and modeled discrimination, assuming that the parameters are accurate, is attributed to g_m. Mesophyll conductance causes a drawdown of CO_2 from the intercellular spaces to the chloroplast.

Mesophyll conductance is important because it can be a significant limiting factor on photosynthesis (Peguero-Pina et al. 2012). Though many photosynthesis models assumed infinite g_m and gas exchange studies did not include g_m, our understanding of g_m is increasing as technology advances (Flexas et al. 2008).

Instantaneous measurements of carbon isotope discrimination for estimating mesophyll conductance were first conducted by Evans et al. (1986). They trapped the CO_2 exhaust from the leaf chamber of a gas exchange system and measured the isotopic composition using an isotope ratio mass spectrometer (IRMS; Evans et al. 1986). In the following years, other researchers developed systems that coupled gas exchange systems to tunable diode lasers (TDL) to simultaneously measure gas exchange and isotope discrimination (Bowling et al. 2003, Tazoe et al. 2011). Another method has been to collect the exhaust of the gas exchange leaf chamber in a flask or syringe and inject that exhaust into a cavity ring-down spectroscopy laser (Berryman et al. 2011).

Previous studies using a coupled gas exchange and online carbon isotope discrimination system noted several challenges (Pons et al. 2009). First, there must be a sufficient CO_2 drawdown by the leaves to get an adequate isotope discrimination signal. This makes working with plants with low photosynthesis difficult. Larger custom leaf chambers or commercial conifer chambers have been used to maximize leaf area. Large leaf chambers are associated with problems such as reduced mixing of air and slower turnover time of the gas in the chamber (Barbour et al. 2007). Low flow rate can also increase the carbon isotope signal, but the flow must be balanced with humidity control in the chamber (Bickford et al. 2009). Another challenge was calibrating the TDL instruments for drift, which could take two hours each sampling day (Bickford et al. 2009). Also, the measurement error must be propagated through calculations of discrimination to ensure that the standard error of the observed discrimination is less than the difference between the observed and modeled discrimination (Douthe et al. 2011). Finally, there are many fractionation and flux parameters in the equations to calculate g_m that are difficult to measure and published values are often used.

The PICARRO G1101-i laser (hereafter, CRDS; Picarro, Santa Cruz, CA) measures $^{12}CO_2$ and $^{13}CO_2$ concentrations in air. It contains an internal cavity which is pressure and temperature controlled. This cavity contains three mirrors, and the effective path length of light is over 20 km. A laser enters the cavity and when the laser is turned off, the light decays because the mirrors are not 100% reflective. Gas inside the cavity absorbs light, and each isotopologue absorbs a unique wavelength. The CRDS measures the decay rates at a scanning rate of 1Hz, and alternates between measurements of $^{12}CO_2$

and $^{13}CO_2$ about every eight seconds (Woelk). CRDS output is in isotope ratios, and it has a $\delta^{13}C$ precision of less than 0.3‰ for five minute averages.

My objective was to design a system that quantifies carbon isotope discrimination and gas exchange simultaneously using the LI-6400XT gas exchange system (hereafter, LI-6400; LI-COR, Lincoln, NE) to the CRDS laser. I configured a valve manifold for using the CRDS to sample the LI-6400 reference gas line and exhaust from the leaf chamber. I then tested the CRDS accuracy and precision over time using a standard of known isotopic composition. Finally, I explored the averaging period necessary for a stable measurement of gas exchange and carbon isotope analysis of reference and sample gas streams. These measurements were then used to calculate mesophyll conductance.

Methods

Valve configuration

A series of three solenoid valves were used to connect the LI-6400 reference line and leaf chamber exhaust to the CRDS using Bev-a-line tubing (polyethylene, lined with ethylene vinyl acetate; LI-COR, Lincoln, NE; Figure 1). The valves were controlled through the CRDS user interface. They were configured to allow the user to switch between analyzing the LI-6400 reference air and the exhaust from the leaf chamber. All air passed through a magnesium perchlorate water trap in the line directly before entering the CRDS.

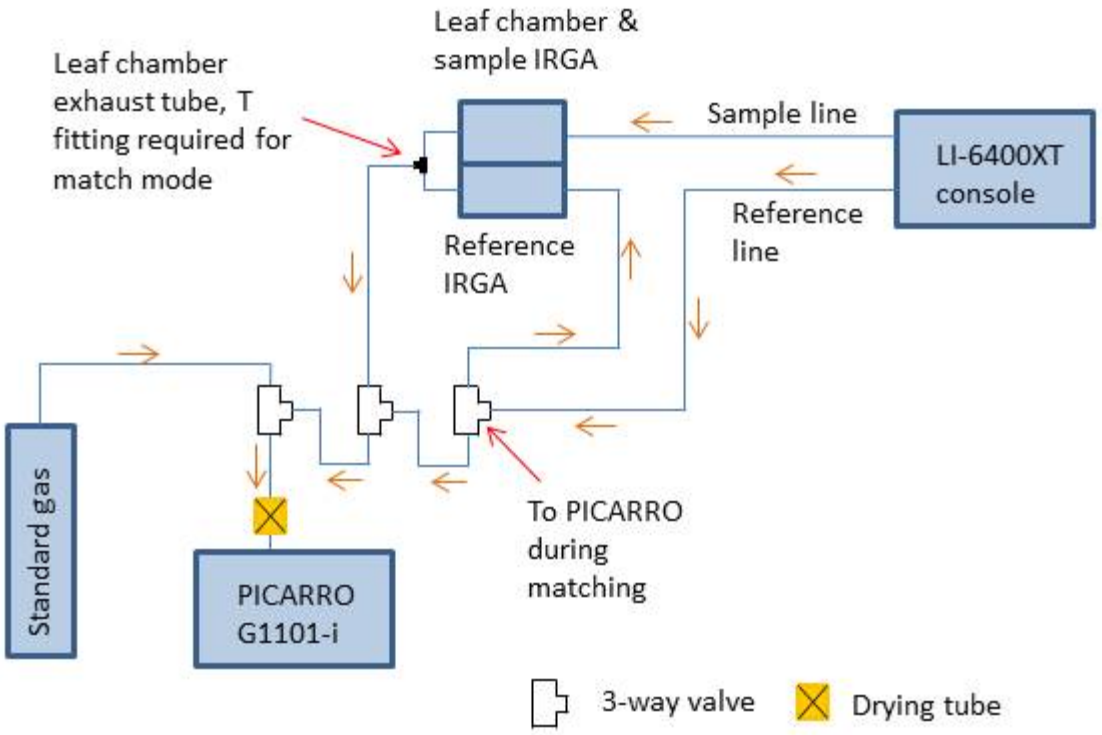

Figure 1. Schematic of system coupling a gas exchange system and cavity ring-down spectroscopy laser.

Testing drift and error

To evaluate the CRDS accuracy and drift over time, a gas of known isotopic composition was analyzed for eight hours, the typical length of a measurement day. A Tedlar bag was filled with -3.57‰ CO_2 standard gas (OzTech, Fremont, CA) and N_2 was added to bring the mixture to a CO_2 concentration of about 150 ppm. A three-way polycarbonate Luer stopcock (Cole-Parmer, Vernon Hills, IL) was connected to the Tedlar bag valve by tubing (Nalgene). First, all air in the bag was evacuated using a vacuum pump. Next, the CO_2 standard tank was connected to the three-way stopcock by

tubing. Using two Swagelock valves on the CO_2 standard tank connected by a short piece of steel tubing, the CO_2 standard tank valve was opened and allowed to diffuse into the steel tubing for five to ten minutes to reach equilibrium. The standard tank valve was then closed and the valves to the Tedlar bag were opened and allowed to diffuse for another five to ten minutes. The valves were then closed and the bag was connected to an ultra-pure N_2 tank and filled to capacity. The bag was then connected to the CRDS and analyzed.

Testing CO_2 concentration accuracy and precision

A cylinder of known CO_2 concentration, 300 ppm (Air Liquide, Plumsteadville, PA), was connected directly to the CRDS intake. Pressure was regulated on the cylinder. Data was recorded for two hours. The $^{12}CO_2$ and $^{13}CO_2$ were summed for a total CO_2 concentration, $[CO_2]$.

Testing CO_2 concentration agreement between CRDS and LI-6400

A buffer volume of ambient air was attached to the LI-6400 intake valve and the LI-6400 reference gas line was connected directly to the CRDS intake. The clocks on both instruments were synced, the LI-6400 IRGAs were matched, and the LI-6400 was set to log data every 30 seconds. The LI-6400 chamber was empty and closed. The LI-6400 sample IRGA and the CRDS both measured the gas stream from the LI-6400 console. The $[CO_2]$ from each instrument was examined. The concentration values of $^{12}CO_2$ and $^{13}CO_2$ from the CRDS were summed for the total $[CO_2]$. The objective was to determine if the concentrations were offset in value or time.

Measurements

The daily start-up procedure began with warming up the CRDS and the LI-6400. The CRDS automatically runs a warm-up and calibration protocol on start-up. This protocol includes allowing the warm box to reach operating temperature, starting gas flow and locking the cavity pressure, calibrating the wavelength monitor, allowing the cavity to reach operating temperature, and starting the spectral analysis program. The procedure usually takes an hour, unless the instrument has recently been on. The LI-6400 also required a start-up procedure. First, the buffer volume of ambient air was connected to the intake valve. The instrument was turned on and the IRGAs were warmed up during the next steps of the start-up protocol. The block and leaf temperature readings, thermocouple, light sensors and PAR values were checked to ensure that they were responsive and gave reasonable values. The leaf fan and flow control were checked. The IRGAs were zeroed. The chamber was checked for leaks and the IRGAs were matched. When both instruments were on, the clocks on each were synced so that data could be compared for specific time intervals.

The needle chamber (LI-6400-07; Li-Cor, Lincoln, NE, USA) was used in order to increase the leaf surface area in the chamber. The chamber dimensions were 2 cm by 6 cm and the top and bottom were clear Propafilm. The chamber did not have a light source, so a 300-Watt LED light panel was positioned above the chamber so that the light at the leaf surface was approximately 900-1100 μmol m^{-2} s^{-1}. The chamber temperature was within 3°C of ambient temperature.

When the reference gas line was diverted to the CRDS for measurement, the LI-6400 was set in match mode, which causes both IRGAs to measure the leaf chamber gas. This prevented the LI-6400 from adjusting the CO_2 concentration due to the reduced air flow to the reference IRGA. It also allowed matching the IRGAs before each plant gas exchange measurement.

The LI-6400 IRGAs measured the CO_2 and H_2O concentrations of air entering the leaf chamber (reference line) and that of air exiting the leaf chamber, as the leaf assimilated carbon and transpired H_2O. Flow was also controlled and recorded from the LI-6400. A buffer volume of ambient air was attached to the LI-6400 intake.

There was a three-minute period after switching the valves until the CRDS raw delta value equilibrated. The length of connections between instruments was minimized to reduce the lag period gas entering the CRDS. The transitions time between sample gases is inherent to the CRDS as it is configured, but removing background tracking and adding faster scanning can reduce this equilibration period (Rella).

The LI-6400 reference gas was measured for six to ten minutes on the CRDS. Then, the valves were switched to measure the sample gas for 15 minutes, while also logging the gas exchange data every 30 seconds on the LI-6400 (Figure 2).

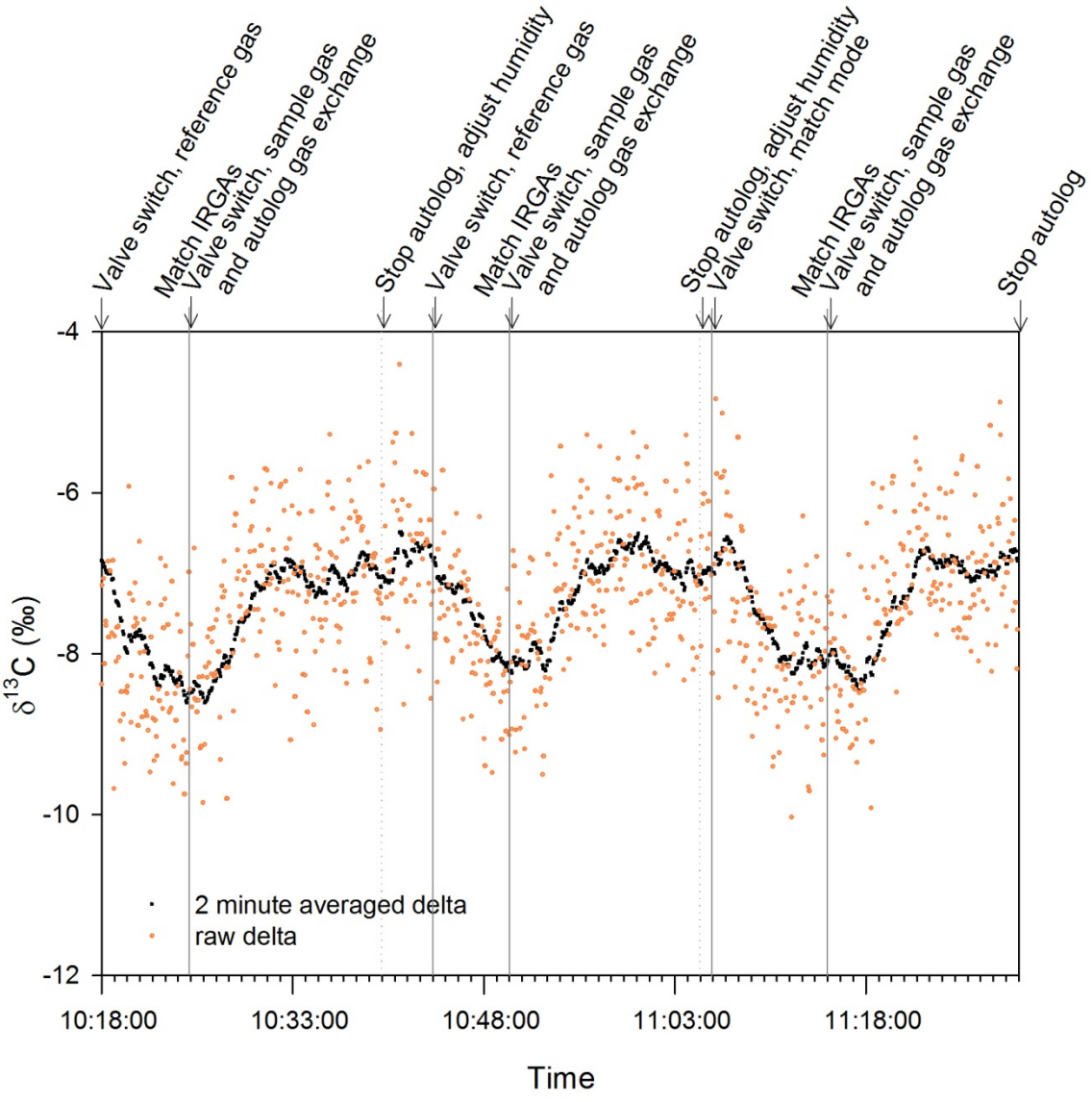

Figure 2. Sequence of events for measurement of gas exchange and carbon isotope discrimination at three different humidity levels for a single plant.

Calculations

Gas exchange data were averaged over the 15 minute period. This included photosynthesis (A), internal CO_2 concentration (C_i), and ambient CO_2 concentration

(C_a). The last four minutes of reference gas data from the CRDS was averaged for the reference CO_2 concentration and carbon isotope composition (C_{ref} and $\delta^{13}C_{ref}$, respectively). This allowed the instrument to stabilize for six minutes. The two minute average δ was examined to ensure that the data included in the average C_{ref} and $\delta^{13}C_{ref}$ was stable. Stability after switching between sample gases was defined when the two minute average δ was no longer changing directionally. The last ten minutes of sample gas data from the CRDS were averaged to get the sample CO_2 concentration and carbon isotope composition (C_{sam} and $\delta^{13}C_{sam}$, respectively). This allowed the instrument to stabilize for five minutes.

The observed discrimination (Δ_{obs}) was calculated following the equation from Evans and von Caemmerer (2012): $\Delta = \frac{1000\xi(\delta^{13}C_{sam}-\delta^{13}C_{ref})}{1000+\delta^{13}C_{sam}-\xi(\delta^{13}C_{sam}-\delta^{13}C_{ref})}$ where $\xi = \frac{C_{ref}}{(C_{ref}-C_{sam})}$, measured by the CRDS.

The predicted discrimination was calculated by first calculating the predicted $\delta^{13}C$ of the plant from the Farquhar simple model: $\delta^{13}C_{pred} = \delta^{13}C_{ref} - a - (b-a) * (\frac{C_i}{C_a})$ where the $\delta^{13}C_{ref}$ is that of the source, measured by the CRDS, a is the fractionation associated with diffusion, 4.4‰, b is the fractionation associated with carboxylation, 29‰, and C_i and C_a are measured by the LI-6400. The modeled discrimination (Δ_i) was calculated by $\Delta_i = \delta^{13}C_{ref} - \delta^{13}C_{pred}$.

Finally, g_m was calculated by the equation found in Barbour et al. (2010), modified from Evans et al. (1986): $g_m = \frac{\left(b-a_l-b_s-\frac{e'R_d}{A+R_d}\right)A}{C_a(\Delta_i-\Delta_{obs})}$, where b= 29‰, a_l is the

fractionation during liquid phase diffusion, 0.7‰, b_s is the fractionation during dissolution of CO_2, 1.1‰, e' is the fractionation associated with mitochondrial respiration in the light, -0.5‰, A is net photosynthesis, and R_d is mitochondrial respiration in the light.

Results

Testing drift and error

The raw delta measurements of the Tedlar bag filled with -3.57‰ CO_2 ranged from -18.76 to 7.25‰ over the entire eight hour period, with an average of -3.50‰ and a standard deviation of 4.20 (Figure 3). The two minute averaged delta values ranged from -6.30 to -1.51‰, with an average of -3.53‰ and a standard deviation of 0.72‰. Over each hour, the standard deviations for the raw delta were similar for the entire period, ranging from 4.00 to 4.28‰, but the standard deviations of two minute averaged delta over hourly periods was lower than that of the entire eight hour period, ranging from 0.40 to 1.02‰ (Figure 4). Standard deviations of two minute averaged delta values over ten minute intervals ranged from 0.31 to 0.50‰.

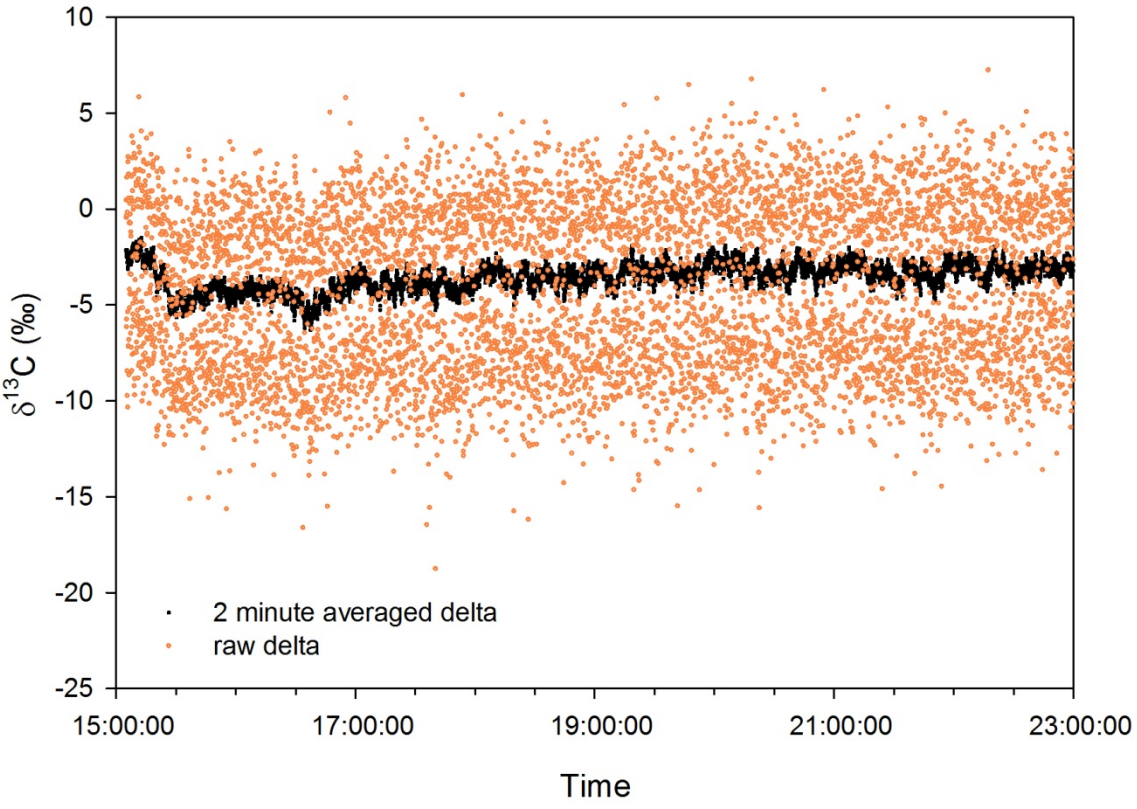

Figure 3. $\delta^{13}C$ of standard gas over an eight hour period.

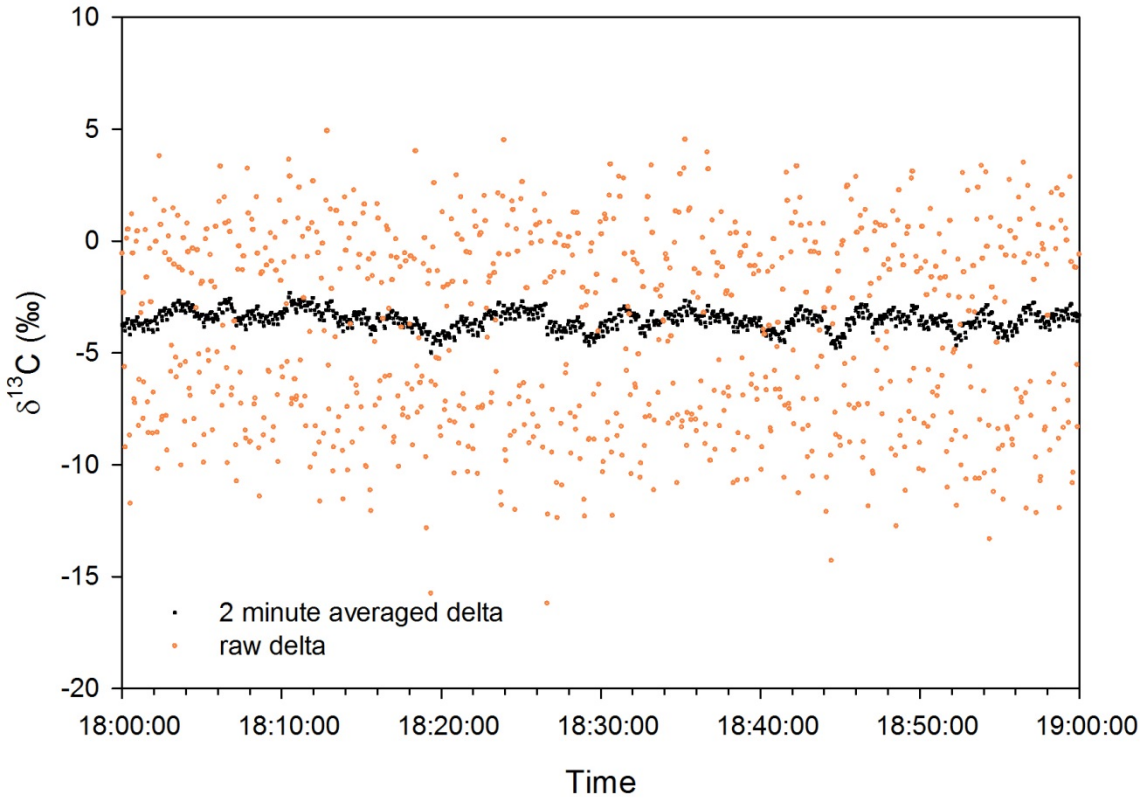

Figure 4. $\delta^{13}C$ of standard gas over a one hour period.

Testing CO_2 concentration accuracy and precision

Over the 1.75 hour period of analyzing a standard tank of 300 ppm CO_2 gas, the CRDS [CO_2] measurement ranged from 299.37 to 301.01 ppm (Figure 5). It averaged 0.38 ± 0.005 ppm higher than the standard tank value.

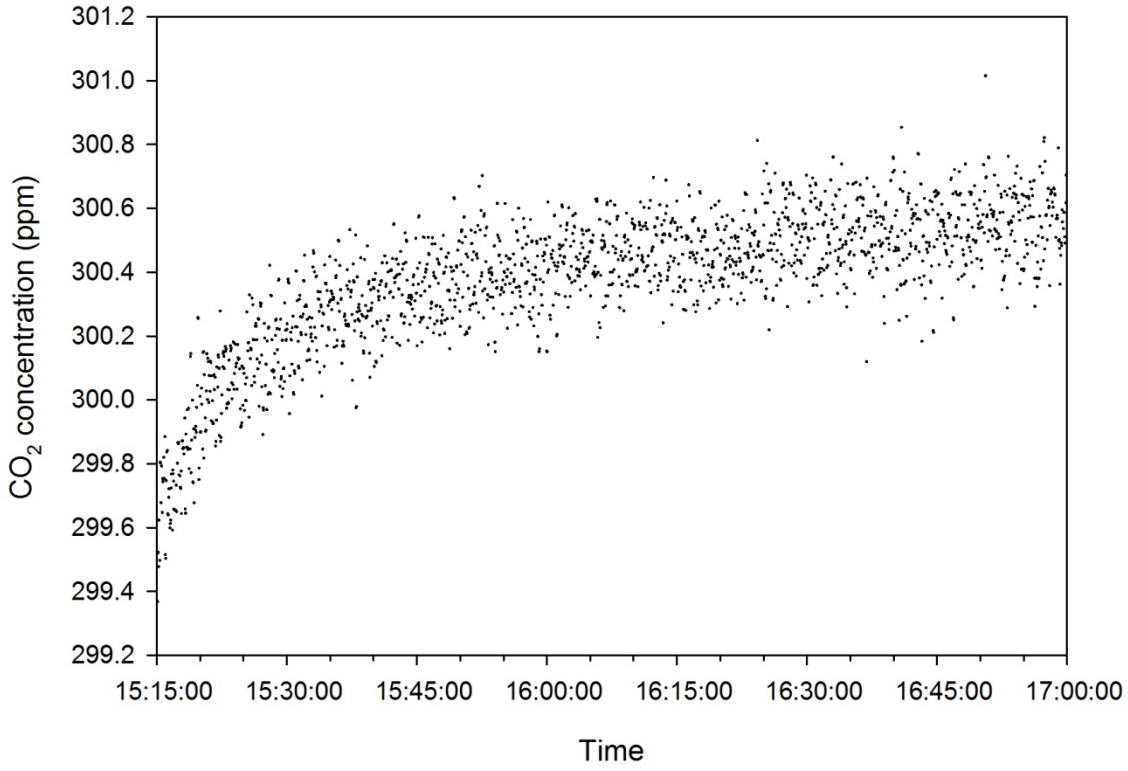

Figure 5. Testing CO_2 concentration measurement accuracy of standard gas, 300 ppm.

Testing CO_2 concentration agreement between CRDS and LI-6400

The [CO_2] measurement by the CRDS was generally lower than that of the LI-6400 sample IRGA but tracked changes similarly across time (Figure 6). Over the 3.25 hour period, the CRDS [CO_2] measurement was lower than the LI-6400 measurement by 4.69 ± 0.22 ppm on average. The transient [CO_2] spikes caused the largest difference between instruments, with the CRDS reaching maximums of 32.7 ppm above the LI-6400 and 52.4 ppm below the LI-6400. Over a two-hour period without spikes in

concentration, the maximum difference between measurements was much lower. In this two-hour period, the average difference was 5.43 ± 0.06 ppm with CRDS reaching a maximum of 9.3 ppm below the LI-6400 and never reporting a value higher than that of the LI-6400.

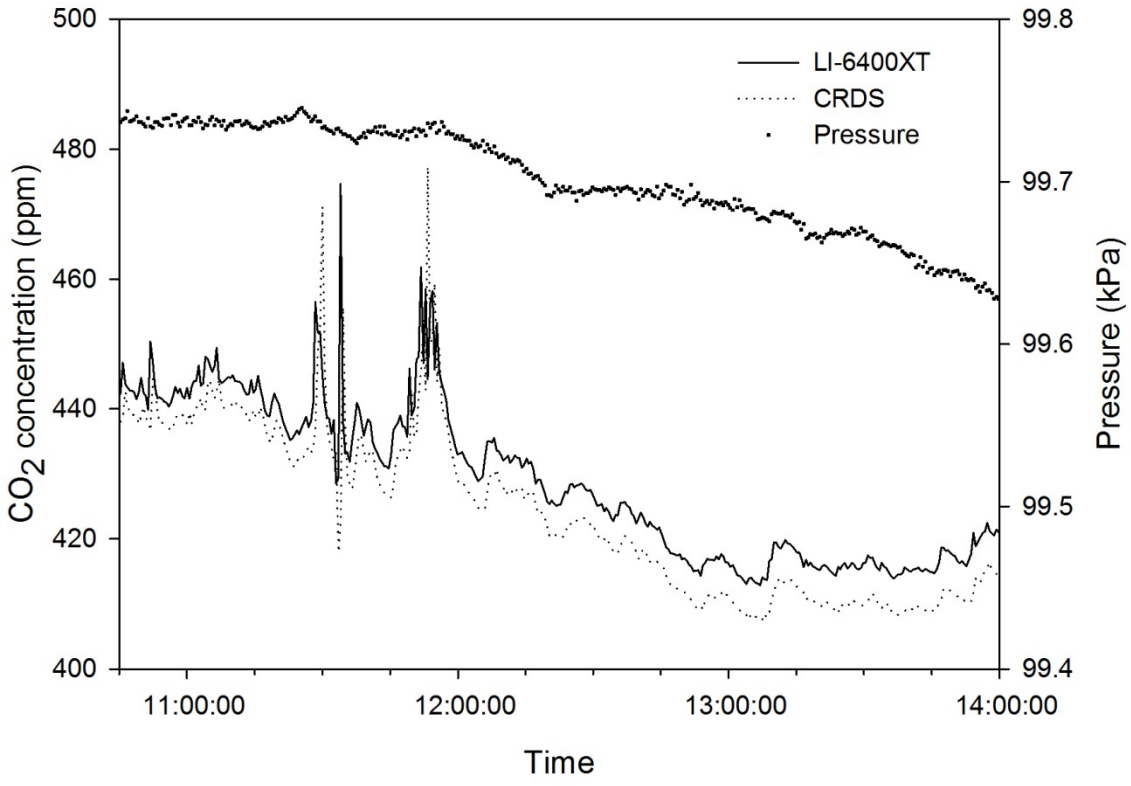

Figure 6. Comparison of CO_2 concentration measurements by LI-6400 and CRDS over time. Leaf chamber was empty and the CRDS measured the reference gas stream.

Calculations of g_m

Mesophyll conductance was calculated from well-watered plants in varying leaf chamber humidity conditions on four measurement days. The decline in [CO_2] of air entering and exiting the leaf chamber due to photosynthesis averaged 22.9 ± 1.13 µmol mol^{-1}. Raw $\delta^{13}C$ of the reference gas stream ranged from -11.7 to -8.08‰, averaging -9.4 ± 0.15‰. Raw $\delta^{13}C$ of the sample gas exiting the leaf chamber ranged from -11.0 to -6.8‰, averaging -8.5 ± 0.18‰. The difference between reference and sample raw $\delta^{13}C$ averaged 0.82 ± 0.05‰. Calculated discrimination ranged from 5.9 to 39.7‰, averaging 18.9 ± 0.90‰.

Photosynthesis averaged over fifteen minutes for each sample ranged in value from 3.0 µmol m^{-2} s^{-1} to 8.2 µmol m^{-2} s^{-1}, and the standard deviations for the averaging periods ranged from 0.07 to 0.28. C_i ranged from 164.2 µmol mol^{-1} to 273.5 µmol mol^{-1}, and the standard deviations for the averaging periods ranged from 0.87 to 6.21, with one standard deviation outside this range at 18.23.

One value of g_m was excluded from analysis as an outlying value. Negative values were included in the analysis, even though g_m cannot be negative, because it was assumed that negative values can give information about the relative differences between clones if there is some offset or error in the measurements. Mesophyll conductance ranged from -0.74 to 0.99 mol m^{-2} s^{-1} (Figure 7). There were no significant effects of clone or block on g_m. Across treatments, the mean g_m was 0.07 ± 0.04 mol m^{-2} s^{-1}.

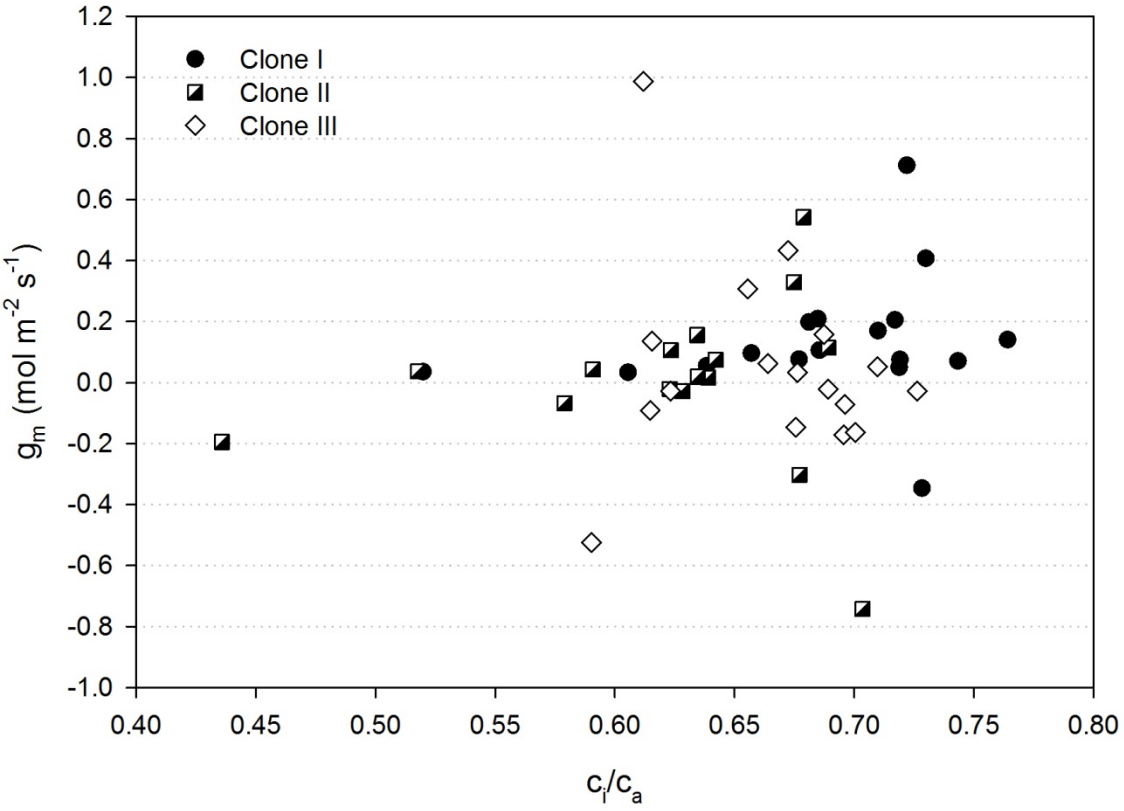

Figure 7. Mesophyll conductance estimated from coupled gas exchange and carbon isotope discrimination measurements at varying humidity levels.

Discussion

The coupled gas exchange and carbon isotope discrimination system described here provided simultaneous measurements of $[CO_2]$, $\delta^{13}C$, A, and C_i. These measurements were used to calculate g_m at a range of C_i/C_a.

The CRDS raw delta measurements had large standard deviations, but averaging over two or five minutes reduced the error. The time necessary for a single round of measurements, including an equilibration time of three minutes after switching valves

and averaging raw data for two to five minutes, was much longer than the measurement cycles of systems that used a TDL. TDL measurements have been made on 20-second or 45-second intervals (Bickford et al. 2009, Douthe et al. 2011, Tazoe et al. 2011). Deviation from the isotopic value of a standard gas showed no consistent increase or decrease over a one-hour period or an eight-hour period, so the discrimination values should not be affected by the length of measurement cycles.

The coupled CRDS and LI-6400 reported [CO_2] values offset by about 5.4 ppm, but the changes in [CO_2] were synced closely in time. The three-minute period between gas samples when switching valves required narrowing the time period for calculating an average delta value for each sample. The three-minute lag period for isotope values was similar to that reported by PICARRO when switching between samples of different [CO_2] (Rella). Needles were left intact on the tree during measurements because each tree was measured for approximately 1.5 hours.

Measurements were originally conducted using a CO_2 cartridge (Li-Cor, Lincoln, NE) with an isotopic composition close to -33‰. Values calculated for discrimination were higher than expected, and switching to ambient air improved the discrimination calculations. The low isotopic composition of the CO_2 cartridges may reduce the accuracy of δ from the CRDS or the plant combined fractionations of photosynthesis and respiration may respond to the low δ with discrimination different than ambient. It is suggested that further measurements be performed with ambient air.

When the LI-6400 entered match mode and the solenoid valves were switched to measure the reference gas line on the CRDS, an error message appeared on the LI-6400

that the sample IRGA value changed by 5-12 ppm. Further testing should be performed to determine if there is a leak or a problem with the valve system. The valves could be causing changes in pressure or the CRDS pump could be causing air to be vacuumed from the leaf chamber. Increasing the flow rate from the LI-6400 did not solve the issue.

Leaves with thick veins increase the likelihood of leaks from the LI-6400 chamber, so needles are also likely to cause leaks. Although the system was checked for leaks with each new sample by breathing around the chamber, putty could be added around the needles to provide an additional seal. Terostat has been used for this application (Tazoe et al. 2011).

The leaf area inside the 2 cm by 6 cm needle chamber was large enough for a sufficient drawdown of CO_2 by photosynthesis only in well-watered plants. With well-watered plants, a significant difference was seen in isotopic composition between the reference and sample air. Plants under water stress could not be used for this analysis. Mesophyll conductance calculations may be more precise with a larger, custom leaf chamber (Pons et al. 2009).

I expected g_m to correlate to C_i/C_a because it has been shown to vary in conjunction with g_s (Douthe et al. 2011). However, there was no correlation between g_m and C_i/C_a in well-watered plants. The average value of g_m calculated here, 0.07 ± 0.04 mol m^{-2} s^{-1}, is similar to that reported for other evergreen conifers (Flexas et al. 2008).

Introduction

The loblolly pine plantation ecosystem in the Southeastern US is unique and presents several advantages as a system for studying g_m. *Pinus taeda* is a long-lived and economically important species with a large body of scientific work on its ecophysiological traits, and many of its genetic lines are known and deployed across a wide geographic region (Baltunis et al. 2008). In addition, its genome is currently being sequenced. According to the EPA, forests and harvested wood in the United States sequestered 834 Tg of CO_2 Eq. (277 Tg C) in 2011, about 12% of the total U.S. greenhouse gas emissions (U.S. Environmental Protection Agency 2013). In addition, well-established extension networks in the Southeast facilitate implementing scientific recommendations for increased C sequestration. For these reasons, the forestry industry is in a unique position to improve management and genetic lines to insure continued productivity as the climate changes. Furthermore, it has the capability to be a significant industry in mitigating climate change through carbon sequestration.

Stomatal conductance is sensitive to drought stress in loblolly pine (Wertin et al. 2012). However, loblolly pine can become conditioned, or acclimated, to drought. Trees exposed to water stress have been seen to respond to a subsequent period of drought stress by maintaining photosynthesis at lower Ψ (Seiler and Johnson 1988). Drought conditioning also improves WUE under well-watered conditions (Seiler and Johnson 1988), but both responses result in lower primary productivity.

Loblolly pine exhibits phenotypic plasticity of water use traits, including xylem resistance to cavitation, in response to different soil textures (Hacke et al. 2000). In addition, stomatal control and hydraulic conductivity have been reported to "act in concert" to limit water loss in loblolly trees as soil water availability declines (Domec et al. 2009). Aspinwall et al. (2011a) found significant genetic control but also high plasticity in both gas exchange and resistance to cavitation in loblolly pine.

A complete understanding of the genetic control on WUE and leaf physiology in loblolly pine has been improving. Significant genotypic differences in $\delta^{13}C$ have been found (Aspinwall et al. 2011b), but the genetic control on carbon isotope discrimination has been unclear and recognized as complex (González-Martínez et al. 2008). There are many genes that each have a small effect on $\delta^{13}C$, height and %N in loblolly pine, and marker-trait associations have been identified for these traits (Cumbie et al. 2011). In addition, it has been reported that instantaneous WUE (from gas exchange, A/g_s) of loblolly pine may have different patterns than the WUE differences indicated by foliar $\delta^{13}C$ such that family differences are exhibited in WUE from $\delta^{13}C$ but not in WUE_i (Yang et al. 2002). WUE from $\delta^{13}C$ may not match WUE_i for several reasons, including the evaporative demand, the temporal and spatial scale of the measurements, and mesophyll conductance (Seibt et al. 2008).

Loblolly pine growth responses are not always explained by leaf physiology. For example, growth response to fertilization may not correlate with changes in A_n (King et al. 2008). There is evidence for genetic control on the response of loblolly trees to fertilization in changes of A_n or biomass allocation (King et al. 2008, Stovall et al.

2013). Recent work with loblolly clones has shown that g_s and A/g_s do not differ among genotypes but A_n does (Aspinwall et al. 2011b). Further research of the controls on growth should be continued with clonal material.

In a greenhouse study, loblolly pine clones were grown under well-watered and drought conditions. The purpose of my study was to examine the physiological and growth responses of loblolly pine to drought. Specifically, I was interested in three components of plant water use and carbon assimilation: stomatal conductance, mesophyll conductance, and hydraulic conductivity, and how these traits relate to growth and productivity. Stomatal conductance and hydraulic conductance have been well studied, but the genetic control and drought effect on mesophyll conductance in loblolly pine in unknown. I used seedlings of three different clones to compare differences in genetic control over the traits of interest.

I hypothesized that 1) structural and physiological traits would be coordinated with each other and growth. I expected the clone that had the fastest growth would exhibit high hydraulic conductivity and cavitation sensitivity to drought, low WUE, and high photosynthesis and mesophyll conductance. A clone with a more conservative growth strategy would be expected to also have lower hydraulic conductivity and increased resistance to cavitation, high WUE, and moderate photosynthesis and mesophyll conductance. I also hypothesized that 2) drought would decrease mesophyll conductance in loblolly pine, but it is unknown if the plasticity of g_m in response to drought will vary by clone.

Methods

Experimental design

Three different clones of *Pinus taeda* L. (loblolly pine) were propagated by somatic embryogenesis and donated by Weyerhaeuser in Hot Springs, Arkansas. Thirty plants from each clone were selected and planted in tree pots (47.75 cm height by 18 cm width) in horticulture media (LC1, Sun-gro, Agawam, MA, USA) and grown in a glasshouse in College Station, TX. The potting media was composed of sphagnum peat moss, perlite, starter nutrients and dolomitic limestone and mixed to a uniform bulk density of 0.0683 g cm^{-3}. Approximately 0.35 cu ft (9.875 L) of mix was used in each pot. The seedlings were planted on January 11, 2013. The trees were hand-watered on the day they were planted and daily as needed for adequate well-watered conditions. The trees were spaced out and arranged in a randomized complete block design replicated ten times. Drip irrigation with ½ gallon per hour emitters was installed to each plant. The plants were fertilized on February 21, 2013 with 1 level Tbsp of Osmocote classic 13-13-13 as a topdressing and 60 mL solution of Hummert's Dyna Green Soluble Trace Elements (dissolved at a rate of 1 oz per 15 gallons of water). The irrigation was reduced to once a week to let the soil dry out between watering to avoid fungal growth on the soil and tree stem. The trees were fertilized with the Soluble Trace Elements solution on April 18 and July 24, 2013.

Water treatments were equal for all plants until May 5, 2013. Water treatments were initiated at this point. The well-watered treatment was irrigated every one to three weeks to maintain higher soil moisture content than the drought treatments. The

moderate drought treatment received no water for a period of nine weeks and the severe drought treatment received no water for a period of ten weeks, during which measurements were made.

Photosynthetically active radiation (PAR) was measured using a quantum sensor (LI-190, Li-Cor, Lincoln, NE, USA). High and low half-hourly air temperature and relative humidity were measured (HMP45AC, Campbell Scientific, Logan, UT, USA) and recorded with a datalogger (CR10X, Campbell Scientific, Inc.). Temperatures in the greenhouse were modulated by pad-and-fan cooling and a heater. A shade cloth covered the greenhouse roof.

Daily maximum temperature ranged from 19 to 41°C with a mean maximum temperature of 31.8°C, and daily minimum temperatures ranged from 10°C to 26°C with a mean minimum temperature of 21.5°C. Humidity at midday ranged from 17% to 95%, with a mean of 60%. Average midday PAR in sunny conditions was 1019 (± 8) μmol s^{-1} m^{-2} in June.

Soil water content was measured continuously with ECHO EC-5 probes (Decagon, Pullman, WA, USA) on a subset of pots with five probes per water treatment, or fifteen total.

Plant growth measurements

Seedling height and diameter were recorded on February 9, May 3, June 11, July 26, and November 15, 2013. Needle length and number of branches were recorded on April 4, May 13, June 11, July 26, and November 15, 2013. One sample was missing because the plant had not received fertilization at the beginning of the experiment.

Height was measured from soil to the rim of the pot and from rim of the pot to the apical bud, and these two measurements were summed. Diameter was measured with a digital caliper reader in two perpendicular directions (N/S and E/W, consistent through all dates) and the average was calculated. Needle length was measured on an intact needle of each flush using a ruler.

Height and diameter were related to final biomass by the equation $B = D^2 * H$, where B is final biomass in g, D is final diameter in cm, and H is final height in cm. Linear regressions were fit to the equation for each clone, and the slopes were significantly different (appendix, $p<.0001$).

Relative rates of change in biomass (RGR) were calculated using equation $\frac{(lnG2-lnG1)}{t2-t1}$ where G1 and G2 are the calculated biomass at time points t1 and t2. Results are shown for the period May to June.

Soil gravimetric water content and bulk density analysis

Pots with soil media and one tree were watered on April 10, 2013 until water drained from the bottom to reach field capacity and were left to drain overnight. At 9:30 AM, 60 mL samples of soil volume were collected for gravimetric water content. The soils were weighed at field capacity, dried for two days at 60°C, and then weighed again. Bulk density was determined as the dry soil mass divided by the volume. Gravimetric water content was determined as the soil water content multiplied by the soil bulk density.

Greenhouse measurements

Pre-dawn water potential (Ψ_{PD}), mid-day water potential (Ψ_{MD}), and gas exchange measurements were made on June 20, 2013 on clones 1, 2, and 3 from blocks 1, 3, 6, and 10. This was 46 days after water treatments were initiated. Pre-dawn measurements were made between 3:00 and 4:30 AM. Ψ_{MD} and gas exchange were measured between 11:00 AM and 2:00 PM. Ψ was measured using a pressure chamber (PMS Instrument Company, Corvallis, OR) on a fascicle. The pressure was recorded when water first appeared on the end of the fascicle. Gas exchange was measured using the LI-6400 with a 2 cm by 3 cm cuvette and blue-red LED light source (LI-COR, Lincoln, NE) on two fascicles (six needles) of first flush growth still attached to the tree. CO_2 was set to 400 ppm and PAR was set to 1500 µmol m^{-2} s^{-1}. Leaf area was determined by measuring the fascicle radius from one needle per fascicle with a digital caliper and calculating the total leaf area with the equation $A_s = N\left(\frac{1}{3} * 2\pi r\right) + 2(Nr)$ where A_s is the surface area of each needle, r is the radius of the fascicle, and N is the needle length in the chamber, modified from Ginn et al. (1991).

Leaf soluble carbohydrates isotope analysis from greenhouse experiment

Samples were collected and analyzed for carbon isotope values of leaf soluble carbohydrates following the method described by West et al. (2007). Leaf samples were collected on June 27 and July 23, 2013 after 5:00 PM from trees grown in a glasshouse. Fully expanded needles were collected from the first flush of 2013 found on the main stem. Four replicates of each treatment were collected and analyzed (blocks 4, 7, 8, and 9). Five to six fascicles were flash frozen in liquid N_2 immediately following removal

from the tree. Samples were stored frozen with dry ice until they could be placed in a freezer in the laboratory (-20°C). Samples were ground with a freezer mill and stored frozen until they were run through the extraction process. 150-200 mg of sample were weighed and placed in 50 mL centrifuge tubes. 10 mL of deionized water was added to each centrifuge tube and the tubes were briefly placed on a vortex and then placed on a shaker for 45 minutes. Samples were placed in a centrifuge for 15 minutes at 11,500 g, immediately after which the supernatant was collected and passed through a series of ion-exchange columns with Dowex-50 and Dowex-1 resins. Dowex-50 and Dowex-1 were intended to remove amino acids and organic acids, respectively. The sample was then lyophilized. For isotope analysis, 0.2 mg of sample was weighed into tin cups. Subsamples were analyzed with an elemental analyzer (Costech, Valencia, CA) coupled to an isotope ratio mass spectrometer (IRMS; Delta V Advantage, Thermo Scientific, Waltham, MA) located at the Stable Isotopes for Biosphere Science (SIBS) Laboratory at Texas A&M University. Ten percent of the samples were randomly chosen to duplicate (n=24) to assess the within-sample heterogeneity and a standard deviation of 0.09‰ was found. Isotope measurements were normalized using USGS Glutamic Acid 40 and 41 and internal plant standards SIBS-pCo and SIBS-pEc were used as check standards. The measured value of SIBS-pCo, -12.58‰, was close to the consensus value, -12.78‰. The measured value of SIBS-pCo, -39.93‰, was close to the consensus value, -39.88‰. N concentrations were corrected using reference plant standard 1515 Apple Leaves (National Institute of Standards and Technology).

For bulk leaf isotope and nitrogen content analysis, 2mg of dried, milled sample were weighed into tin cups. Subsamples were analyzed with an elemental analyzer (Costech, Valencia, CA) coupled to an IRMS (Delta V Advantage, Thermo Scientific, Waltham, MA) located at the Stable Isotopes for Biosphere Science (SIBS) Laboratory at Texas A&M University. Ten percent of the samples were randomly chosen to duplicate (n=23), and a standard deviation of 0.04‰ was found. Isotope results were normalized using USGS Glutamic Acid 40 and 41 and internal plant standards SIBS-pCo and SIBS-pEc were used as check standards. The measured value of SIBS-pCo, -12.64‰, was close to the consensus value, -12.78‰. The measured value of SIBS-pEc, -39.95‰, was close to the consensus value, -39.88‰. N concentrations were corrected using reference plant standard 1515 Apple Leaves (National Institute of Standards and Technology).

Additionally, on June 27 and July 23, Ψ_{PD}, Ψ_{MD}, and gas exchange were measured. Ψ_{MD} and gas exchange were measured between 11:00 AM and 2:00 PM. Ψ was measured using a pressure chamber (PMS Instrument Company, Corvallis, OR). Gas exchange was measured using the LI-6400XT (hereafter, LI-6400; LI-COR, Lincoln, NE) on two fascicles (six needles) of first flush growth still attached to the tree. Reference CO_2 was set to 400 ppm and PAR was set to 1500 µmol m^{-2} s^{-1}. Leaf area was determined by measuring the fascicle radius from one needle per fascicle and calculating the total leaf area.

Estimation of g_m

A/C_i curve fitting

Six blocks were selected to perform A/C_i curves with the LI-6400. A Latin Square design was used, with the two variables being day and time of day. Gas exchange measurements were made on November 1, 2, 4, 5, 7, and 8, 2013. Ψ_{PD} and Ψ_{MD} were measured for all plants on Nov 6, 2013. Gas exchange was measured on six plants each day, with one plant per hour beginning at 10 AM and ending at 4 PM. A standard 2 cm by 3 cm leaf chamber with LED light was used. Plants were placed under a 300-Watt LED light for an hour prior to needles being placed in the leaf chamber to acclimate to high light conditions. At the start of each day, the LI-6400 was warmed up and calibrated and the IRGAs were matched. PAR inside the chamber was set to 1200 µmol m^{-2} s^{-1}, flow was set to 300 µmol s^{-1}, and block temperature was regulated between 22°C and 24°C to keep the leaf temperature between 24°C and 26°C. Desiccant was partially bypassed to keep the relative humidity between 40% and 70%.

Two fascicles of current year, fully expanded needles were selected on each plant. Some blocks had more mite damage than others, but the impact of mite damage on photosynthesis was accounted for by including block effects in statistical modeling. Healthy needles were selected when possible. The chamber was clamped tighter when needed to reduce leaks around the needles. The gas exchange measurements were made with the fascicles remaining attached to the plant. The needles were placed in the chamber and allowed to acclimate to the light for 20 minutes at CO_2 level of 400 ppm. Measurements were then made at reference CO_2 levels: 400, 300, 200, 150, 100, 50, 30,

400, 600, 800, 1000, and 1400 ppm. Measurements were three minutes apart to allow the conditions to stabilize, and IRGAs were matched before each measurement. After the set of measurements, the fascicle radius from one needle from each fascicle was measured with a digital caliper. Gas exchange data was corrected for the actual leaf surface area.

To correct for diffusion leaks, with an empty chamber, CO_2 and H_2O of the ambient air were measured (open chamber sample measurements). Dried, dead needles were clamped into the chamber. With the desiccant on full scrub and CO_2 at 1950 ppm, flow was set to 500 µmol s^{-1}. When the system was stable, IRGAs were matched and data was logged. The process was repeated for flow rates 250, 125, 100, 75, 60, and 50 µmol s^{-1}.

Using this data, a linear regression was made for $\frac{(C_s - C_r)}{(C_a - C_s)}$ vs. $Flow^{-1}$. K_{CO2} was estimated at 0.18 and K_{H2O} at 4.03. K_{CO2} was then used to correct the photosynthesis measurement by the equation $actual\ photosynthesis = apparent\ photosynthesis + \frac{(K_{CO2} * (C_a - C_s))}{100S}$ where S is the leaf area.

Each corrected A/C_i curve was used to simultaneously solve g_m, V_{cmax}, J, R_d, and Γ* using equations for the RUBISCO and RUBP-regeneration limitations on photosynthesis (Farquhar et al. 1980). Solutions for g_m that were higher than 2 mol m^{-2} s^{-1} were not included in the analysis (seven samples, four of which were clone III in the moderate drought treatment). Three trees yielded data that did not form a standard A/C_i curve. The photosynthesis parameters could not be determined for these three samples and the data was not used. Data were square-root transformed for analysis.

Chlorophyll fluorescence

Chlorophyll fluorescence was measured on light adapted plants with the LI-6400 40 Leaf Chamber Fluorometer (LCF, LI-COR, Lincoln, NE) on November 12, 14, and 15. Dark respiration was measured on November 15, 2013. All measurements were on the same flush as the A/C_i measurements and fascicles remained attached to the plant. Chlorophyll fluorescence was measured at each CO_2 level for the first block, then only at 600 ppm and 800 ppm reference CO_2 for the subsequent blocks because electron transport rate (J) was determined to be highest at these levels, where C_i was closest to 400 ppm. C_i values under 200 ppm are most likely in the RUBISCO-limited phase of photosynthesis, while values above 300 ppm are most likely in the RUBP-regeneration-limited phase (Sharkey et al. 2007). Some plants had very low C_i, most likely caused by stomata closing at the higher CO_2 concentrations or the plant shutting down photosynthesis. Clone I in the moderate drought treatment was unusual in that 3 of the 6 plants had C_i values below 200 ppm. These samples could not be used in analysis because photosynthesis must be limited by RUBP-regeneration for the g_m equation to be valid, and this phase occurs when C_i is above 300 ppm.

Γ^*, the chloroplastic photocompensation point, and R_d, leaf respiration in the absence of photorespiration were calculated following the method by Brooks and Farquhar (1985). Gas exchange was measured on fully expanded needles using the LI-6400. First, an A/C_i curve was constructed at PAR set to 1000 μmol m^{-2} s^{-1}. Measurements were logged at each reference CO_2 point of 400, 300, 200, 150, 100, 50, 400, 500, 600, 700, 800, 900, and 1000ppm. Then, A/C_i curves were constructed at low

CO_2 concentrations and PAR conditions. PAR was set at 400, 300, and 150 µmol m^{-2} s^{-1}. At each irradiance level, measurements were taken at reference CO_2 of 140, 120, 100, 90, 80, 70, 60, and 50 ppm. Data was corrected for leaf area and diffusion as described previously. Linear regressions were made for each set of A/C_i measurements, and the intersections of each set of curves were calculated and averaged. The y-value of the intersection was multiplied by -1 to get R_d. The x-value of the intersection was the estimate of C_i*, the intercellular photocompensation point of C_i. C_i* and Γ* are related according to the equation $\Gamma^* = C_i^* + \frac{R_d}{g_m}$ (von Caemmerer et al. 1994). Thus, Γ* and g_m were estimated iteratively using this equation and simultaneously solving g_m, V_{cmax}, and J for the full A/C_i curve that was constructed at PAR of 1000 µmol m^{-2} s^{-1}.

Mesophyll conductance was estimated from the chlorophyll fluorescence and gas exchange data using the equation from Harley et al. (1992) for the Variable J method, $g_m = \frac{A}{C_i - \left(\frac{\Gamma^*[J+8(A+R_d)]}{J-4(A+R_d)}\right)}$, where A is the net assimilation rate of CO_2 on a leaf area basis from the LI-6400 chlorophyll fluorescence chamber (µmol CO_2 m^{-2} s^{-1}), C_i is the internal CO_2 partial pressure (µbars), Γ* is the chloroplastic photocompensation point (µbars), J is the electron transport rate measured by the LI-6400 40 LCF (µmol m^{-2} s^{-1}), and R_d is the leaf respiration in the absence of photorespiration (µmol CO_2 m^{-2} s^{-1}).

$\delta^{13}C$ of soluble carbohydrates and gas exchange

$\delta^{13}C_{sc}$ was analyzed and gas exchange at saturating light was measured on June 27, 2013 and July 23, 2013, as described previously. Mesophyll conductance was estimated using equations from Barbour et al. (2010). First, the observed discrimination,

Δ_{obs}, was calculated as $\Delta_{obs} = \frac{\delta^{13}C_a - \delta^{13}C_{sc}}{1+\delta^{13}C_{sc}}$ where $\delta^{13}C_a$ was the isotopic composition of the ambient greenhouse air, -8.54‰, an average measured by the PICARRO G1101-i laser (Picarro, Santa Cruz, CA). The modeled discrimination, Δ_i, was calculated by the equation $\Delta_i = a_b \frac{C_a - C_s}{C_a} + a\frac{C_s - C_i}{C_a} + b\frac{C_i}{C_a} - f\frac{\Gamma^*}{C_a} - e'\frac{R_d}{A+R_d}\frac{C_i - \Gamma^*}{C_a}$ where a_b is the fractionation during diffusion through the boundary layer, 2.9‰, C_a was measured by the LI-6400 sample IRGA, C_s was the CO_2 concentration at the leaf surface, calculated by $C_s = C_a - \frac{A}{g_{bl}}$ where g_{bl} is the boundary layer conductance, 2.84 mol m^{-2} s^{-1}, a is the fractionation during diffusion in air, 4.4‰, b is the fractionation during carboxylation by RUBISCO and phospho*enol*pyruvate carboxylase (PEPC), 29‰, f is the fractionation associated with photorespiration, 11.6‰, and e' is the fractionation associated with mitochondrial respiration in the light, -0.5‰. Γ* and R_d were calculated as described previously. A, C_i, C_a, and C_s for each clone by water treatment were averaged and the average was used in the calculation of g_m for each plant. Using the above parameters, g_m was calculated from the equation $g_m = \frac{(b - a_l - b_s - \frac{e'R_d}{A+R_d})A}{C_a(\Delta_i - \Delta_{obs})}$ where a_l is the fractionation during liquid phase diffusion, 0.7‰ and b_s is the fractionation during dissolution of CO_2, 1.1‰. Four values were excluded from analysis for g_m estimated from June $\delta^{13}C_{sc}$ due to values of A or $\delta^{13}C_{sc}$ that were outliers. One value was excluded from analysis for the g_m from July $\delta^{13}C_{sc}$ due to an outlying g_m value.

Online carbon isotope discrimination and gas exchange

Simultaneous gas exchange and carbon isotope discrimination were measured and g_m was calculated according to the methods described previously. Measurements were made on well-watered trees of each clone from four blocks at low, medium and high relative humidity in order to measure g_m over a range of C_i/C_a. Measurements were conducted in the greenhouse on August 1, 21, 26, and September 2, 2013. One value was excluded from analysis due to an outlying g_m value.

Harvest

Plants were harvested on November 18, 2013. The severe drought treatment was not included and nine samples of the moderate drought treatment were missing because the trees had died from drought during the experiment. Ten fascicles from the flush that had been measured for chlorophyll fluorescence were removed from the tree and placed in a bag. Twenty fascicles randomly selected from the whole tree were removed and placed in a bag. These two separate groups of needles were then taped flat and not overlapping to acetate sheets. Each sheet was run through the LAI-1000 three times and an average of the three readings was calculated for leaf area. The needles were then dried in a drying oven at 65°C for 48 hours. Once dry, the mass of the needles was measured. Specific leaf area (SLA) was calculated by the dividing the needle area by the mass. SLA was used to estimate the total leaf area based on the total foliar biomass of each seedling.

The aboveground portion of the tree was cut at the level of the pot and placed in a bag. The soil was shaken off the roots and the roots were rinsed clean in water and

placed in plastic bags and stored in a refrigerator. The stems, branches, and roots were dried in a drying oven at 65° for 72 hours. The dry mass of the stems with branches and dry mass of the roots were measured.

Hydraulic conductance

Four complete blocks were selected for hydraulic conductivity analysis (n=4) and one sample was missing due to mortality, for 23 samples total. Stem sections without branches were cut, stripped of needles, wrapped in moist paper towels, and mailed to JC Domec at Duke University for hydraulic conductivity analysis. Hydraulic conductivity (K_s) and vulnerability to cavitation was measured following Sperry and Saliendra (1994) and Domec et al. (2012) by the air injection technique. Leaf specific conductivity (LSC) was determined from K_s, xylem area, and total leaf area. The dry mass of each stem sample was recorded and added to the aboveground biomass of the tree.

Dry weight

Needles, branches, and stem were separated and dry mass of each portion was measured. Roots were separated as follows: the aboveground portion of the stem was cut at the soil line by visually examining the change in color caused by contact with the soil. The belowground portion was cut at the point where the first lateral root emerged. Each portion was dried at 65°C for 72 hours and subsequently weighed on an electronic balance.

Statistical analysis

Analysis of variance (ANOVA) was performed to determine the statistical significance of water treatment, clone, water treatment by clone interaction, and block effects using JMP v.10 (SAS Institute, Cary, NC, USA). A linear model with main effects clone, water treatment, and block and interaction term clone by water treatment was used. Curve fitting for A/C_i curves was performed in Excel v.14 (Microsoft, Redmond, WA, USA). Treatment effects on growth were analyzed over time with repeated measures analysis using PROC MIXED with block and block-by-treatment included as random effects (SAS 9.4, SAS Institute, Cary, NC, USA). Treatment effects on $\delta^{13}C_{sc}$ were analyzed as a split-block design for two sampling dates. Treatment effects on g_m and LSC and vulnerability to cavitation were examined. Residuals were plotted to confirm that the data met assumptions of equal variance and normality. For g_m, residuals from the model show that the data were not normal. A square-root transformation of the data was performed and analyzed.

Values were identified and excluded as outliers if they were more than two standard deviations away from the treatment mean. Arithmetic means and standard errors are reported, and Tukey's HSD letter differences are shown.

Results

Soil moisture and Ψ_{PD}

Soil moisture varied during the experiment between 25.5% and 0% across treatments. Over the experiment, soil moisture averaged 16.9%, 9.3%, and 3.0% in the

well-watered, moderate drought, and severe drought treatments, respectively (Figure 8). Ψ_{PD} ranged between -0.3 MPa and -4.45 MPa. The well-watered treatment soil moisture declined below 10% four times during the study. It was below 10% soil water content for a period of 12 days and reached a minimum of 2% soil moisture in early to mid-July.

In June, Ψ_{PD} had significant effects by clone ($p<.0001$) and water treatment ($p=0.0023$) but no interaction. Drought significantly decreased Ψ_{PD} from -0.5 ± 0.02 MPa in the well-watered treatment to a low of -1.2 ± 0.11 MPa in the severe drought treatment. Clone I had the highest Ψ_{PD} across treatments, -0.7 ± 0.06 MPa and clone II had the lowest, -1.0 ± 0.13 MPa. Only one of the plants displayed a Ψ_{PD} below -2.0 MPa, which was in the severe drought treatment

July measurements were made under an extended drought period. Ψ_{PD} in July was also significantly different by clone ($p=0.0029$) and water treatment ($p<.0001$) with no interaction. Drought significantly decreased Ψ_{PD} from -0.5 ±0.02 MPa in the well-watered treatment to -2.2 ± 0.22 MPa in the moderate drought treatment and -2.2 ± 0.94 MPa in the severe drought treatment. Clone I had the highest Ψ_{PD} across treatments, -1.1 ± 0.16 MPa and clone II had the lowest, -1.9 ± 0.31 MPa. Twelve of the 36 trees sampled in July had Ψ_{PD} below -2.0 MPa.

Ψ_{PD} in November had a significant water treatment effect ($p<.0001$) with no clone or interactive effects. Drought significantly decreased Ψ_{PD} from -0.4 ± 0.05 MPa in the well-watered treatment to -0.6 ± 0.10 MPa in the moderate drought treatment.

The July measurements were made during a period of extended drought. July Ψ_{PD} had the greatest difference between the well-watered and drought treatments, June was moderately different, and November was small but significantly different.

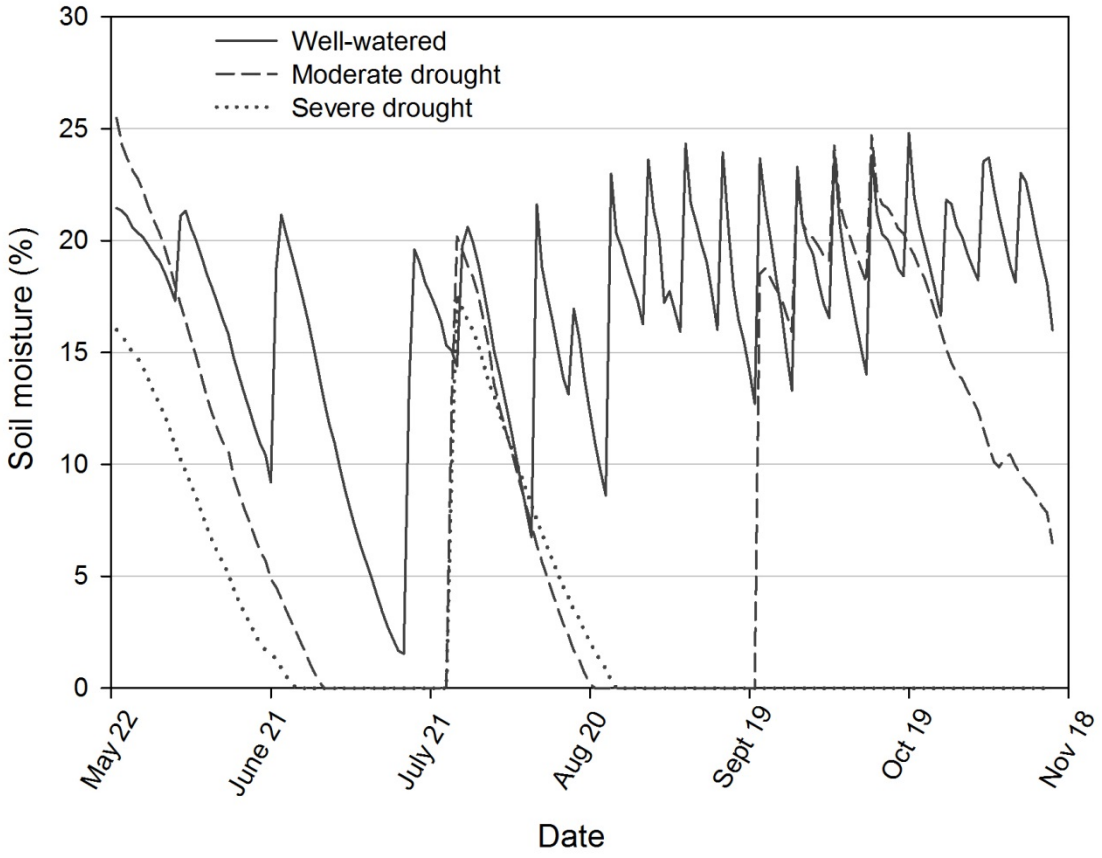

Figure 8. Volumetric soil moisture content (%) from soil probes for well-watered, moderate drought, and severe drought treatments (n=5).

Leaf nitrogen and LMA

In June, clone and water treatment both had significant effects on leaf N, with drought reducing leaf N (clone p=0.0199, water treatment p=0.0217). There was no interaction or block effect. Clone II had the lowest leaf N at 0.94% ± 0.057 and clone III had the highest at 1.10% ± 0.056 across water treatments. Drought reduced leaf N by 8.4% in the moderate drought and 12.3% in the severe drought treatment across clones. However, in July, only the block effect was significant (p=0.0488). Clone was significant at a 90% confidence level (p=0.0545) with averages across water treatments of 0.96% ± 0.027 for clone I, 0.91% ± 0.045 for clone II, and 1.02% ± 0.031 for clone III. Water treatment effect was not significant (p=0.1305).

Net photosynthesis in June had a positive correlation with leaf N (p=0.0001, R^2=0.41) and the best model of A_n included leaf N and water treatment (Figure 9a, R^2=0.83 compared to R^2=0.70 for water treatment alone). Conversely, net photosynthesis in July differed by water treatment (Figure 9b, p<0.0001, R^2=.88) but was unrelated to leaf N% (p=0.3494).

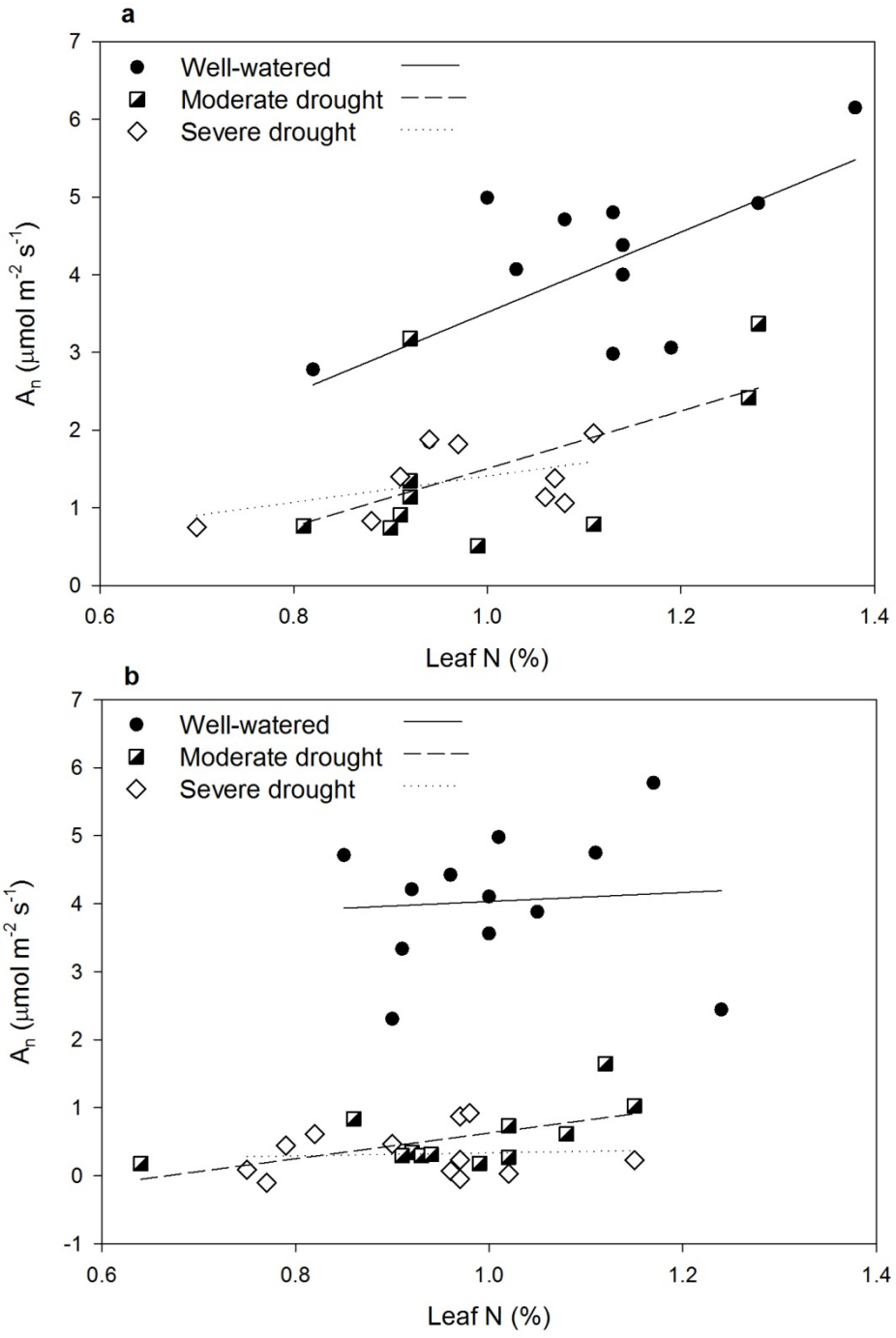

Figure 9. Photosynthesis by leaf nitrogen for each water treatment in (a) June (R^2=0.83) and (b) July (R^2=0.88, significant at $p<0.05$).

LMA did not significantly vary between clones (p=0.1514) or water treatments (p=0.2648), but there was a general trend of LMA increasing by 4.23% across clones under drought stress (Figure 10).

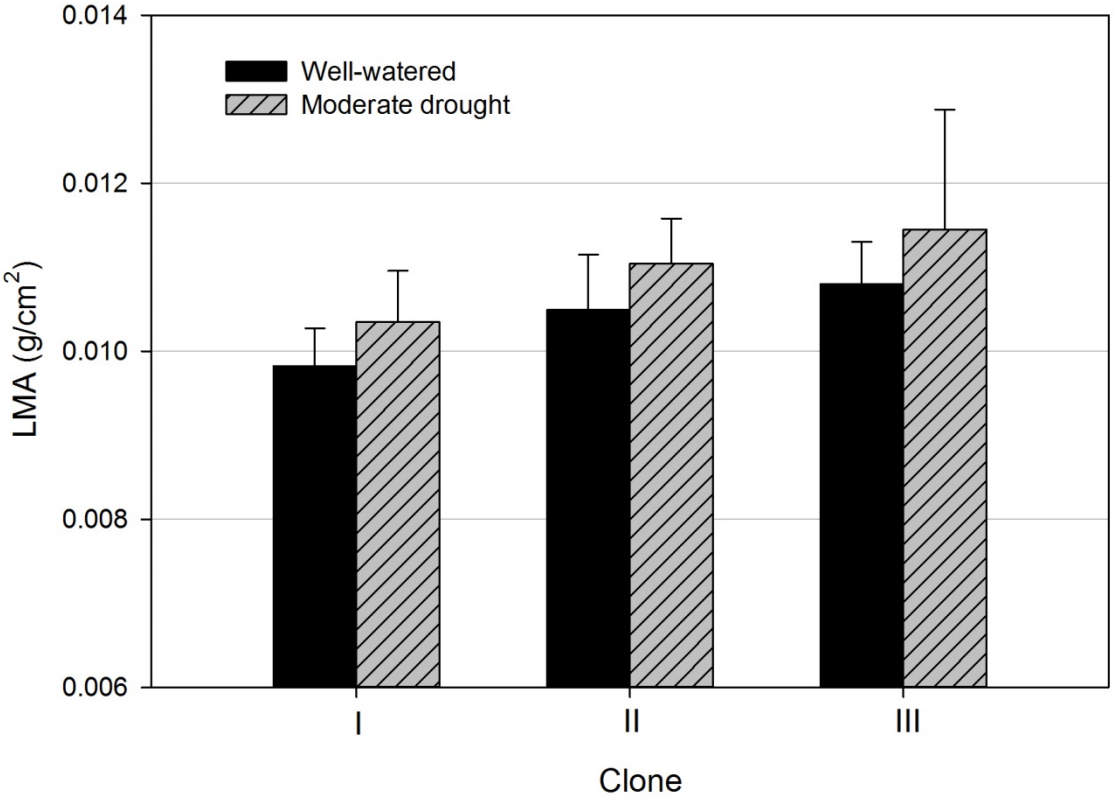

Figure 10. Leaf mass per unit area for well-watered treatment (black bars) of clone I (n=9), clone II (n=7), and clone III (n=9) and moderate drought treatment (dashed bars) of clone I (n=9), clone II (n=4), and clone III (n=7).

Gas exchange

In June, A_n averaged from 4.1 ± 0.35 µmol CO_2 m^{-2} s^{-1} in the well-watered treatment down to 1.2 ± .02 µmol CO_2 m^{-2} s^{-1} in the severe drought treatment (Table 1). Drought significantly reduced A_n ($p<.0001$) by 66.7% in the moderate drought and 70.7% in the severe drought treatment. There were no differences by clone. Stomatal conductance was significantly affected by both water treatment ($p<.0001$) and clone ($p=0.0119$), but there was no interactive effect. Stomatal conductance was 71.9% lower in the moderate drought and 76.5% lower in the severe drought treatment than in the well-watered treatment. Clone III had the highest g_s, 0.046 ± 0.0119 mol H_2O m^{-2} s^{-1} and clone II had the lowest, 0.035 ± .0091 mol H_2O m^{-2} s^{-1}.

In July, A_n averaged from 4.0 ± 0.29 µmol CO_2 m^{-2} s^{-1} in the well-watered treatment down to 0.3 ± .10 µmol CO_2 m^{-2} s^{-1} in the severe drought treatment. Drought significantly reduced A_n ($p<.0001$) by 86.1% in the moderate drought and 92% in the severe drought treatment. There were no differences by clone. Drought significantly reduced g_s ($p<.0001$) by 83.6% in the moderate drought and 82.2% in the severe drought treatment. Stomatal conductance averaged from 0.090 ± 0.0271 mol H_2O m^{-2} s^{-1} in the well-watered treatment down to 0.015 ± 0.0050 mol H_2O m^{-2} s^{-1} in the moderate drought treatment.

In November, no significant effects were seen on A_n, but there was a trend of clone by water treatment interactive effect on A_n ($p=0.0726$). A_n ranged from an average of 4.8 ± 0.73 µmol CO_2 m^{-2} s^{-1} in clone I in the moderate drought treatment down to 2.1 ± 0.55 µmol CO_2 m^{-2} s^{-1} in clone II in the moderate drought treatment. Drought

significantly reduced g_s ($p<.0001$) by 54.0% in the moderate drought treatment. Stomatal conductance averaged 0.071 ± 0.0071 mol H_2O m^{-2} s^{-1} in the well-watered treatment down to 0.033 ± 0.0048 mol H_2O m^{-2} s^{-1} in the moderate drought treatment. There were also differences in g_s by clone ($p=0.0205$), with an average of 0.067 ± 0.0089 mol H_2O m^{-2} s^{-1} in clone I, 0.051 ± 0.0116 mol H_2O m^{-2} s^{-1} in clone II, and 0.038 ± 0.016 mol H_2O m^{-2} s^{-1} in clone III.

Mesophyll conductance

Estimates of g_m varied between methods. Estimating g_m from A/C_i curves, there was a significant effect of water treatment ($p=0.0090$) in which drought increased g_m from 0.12 ± 0.05 mol m^{-2} s^{-1} bar^{-1} in well-watered treatment to 0.30 ± 0.22 mol m^{-2} s^{-1} bar^{-1} in the moderate drought treatment across clones.

From the A/C_i curves at low irradiances, R_d was 0.4015 µmol m^{-2} s^{-1} and Γ* was estimated to be 28.87 µbars. These parameters were used in the variable J method of calculating g_m from chlorophyll fluorescence and gas exchange. There were no treatment effects on g_m measured from chlorophyll fluorescence (Figure 11). The overall mean was 0.022 ± 0.002 mol m^{-2} s^{-1} bar^{-1}.

For the g_m derived from $\delta^{13}C_{sc}$ and gas exchange in June, there was a significant clone effect ($p<.0001$) and clone by water treatment effect ($p<.0001$) on g_m. There were no differences between clones in the moderate drought and well-watered treatments, but clone I in the well-watered treatment had the highest g_m at 0.45 ± 0.14 mol m^{-2} s^{-1} and clones II and III in the well-watered treatment had the lowest g_m at -0.26 ± 0.04 and

Table 1. Gas exchange means and standard errors and ANOVA statistics

	Units	**Clone I**	**Clone II**	**Clone III**	**Well-watered**	**Moderate drought**	**Severe drought**		**Clone**	**Water treatment**	**Clone x water treatment**
A_n, June 27, 2013	µmol CO_2 m^{-2} s^{-1}	2.14 ± 0.446	1.99 ± 0.483	2.57 ± 0.506	4.06 ± 0.345	1.35 ± 0.256	1.19 ± 0.145	F-ratio	1.7697	51.4381	0.5915
								DF	2	2	4
								p-value	0.1928	**<.0001**	0.6722
g_s, June 27, 2013	mol H_2O m^{-2} s^{-1}	0.044 ± 0.0371	0.035 ± 0.0091	0.046 ± 0.0119	0.081 ± 0.0091	0.023 ± 0.0041	0.0191 ± 0.0022	F-ratio	5.4116	67.0221	1.3038
								DF	2	2	4
								p-value	**0.0119**	**<.0001**	0.2980
A_n, July 23, 2013	µmol CO_2 m^{-2} s^{-1}	1.79 ± 0.497	1.63 ± 0.632	1.51 ± 0.501	4.04 ± 0.293	0.56 ± 0.127	0.32 ± 0.100	F-ratio	0.5403	119.3580	1.1713
								DF	2	2	4
								p-value	0.5895	**<.0001**	0.3483
g_s, July 23, 2013	mol H_2O m^{-2} s^{-1}	0.044 ± 0.0127	0.039 ± 0.0114	0.037 ± 0.0102	0.090 ± 0.0078	0.015 ± 0.0014	0.016 ± 0.0014	F-ratio	0.5389	83.3356	0.1839
								DF	2	2	4
								p-value	0.5903	**<.0001**	0.9445
A_n, Nov 2013	µmol CO_2 m^{-2} s^{-1}	4.63 ± 0.387	3.43 ± 0.655	3.28 ± 0.353	4.26 ± 0.380	3.30 ± 0.418	Missing data	F-ratio	2.9019	3.6933	2.9174
								DF	2	1	2
								p-value	0.0736	0.0661	0.0726
g_s, Nov 2013	mol H_2O m^{-2} s^{-1}	0.067 ± 0.0089	0.051 ± 0.0401	0.038 ± 0.0046	0.071 ± 0.0071	0.033 ± 0.0048	Missing data	F-ratio	4.5585	24.9890	1.4126
								DF	2	1	2
								p-value	**0.0205**	**<.0001**	0.2623

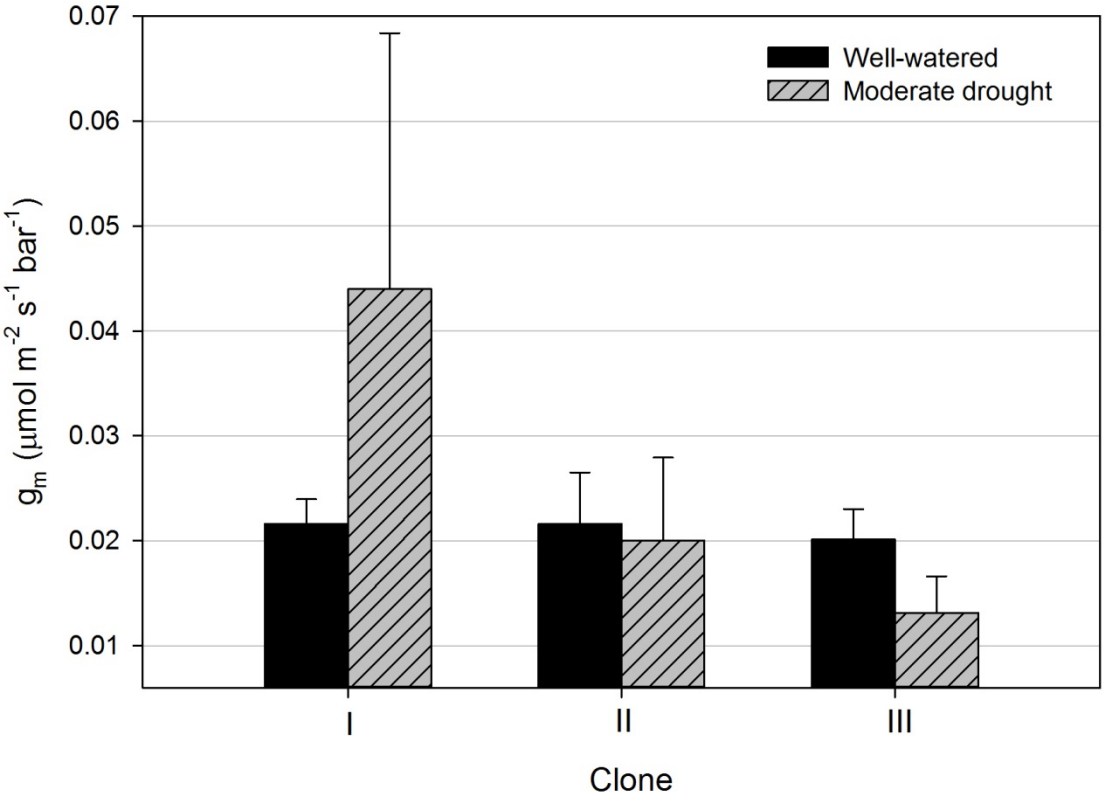

Figure 11. Mesophyll conductance estimated using fluorescence measurements for well-watered treatment (black bars) of clone I (n=6), clone II (n=6), and clone III (n=6) and moderate drought treatment (dashed bars) of clone I (n=3), clone II (n=6), and clone III (n=6).

-0.13 ± 0.01 mol m^{-2} s^{-1}, respectively. The moderate drought and severe drought treatment g_m values averaged 0.06 ± 0.01 and 0.05 ± 0.01 mol m^{-2} s^{-1}, respectively.

For the g_m derived from $\delta^{13}C_{sc}$ and gas exchange in July, there were no significant effects of clone or water treatment on g_m. Across treatments, the mean g_m was -0.04 ± 0.04 mol m^{-2} s^{-1}.

For the g_m derived from online gas exchange and carbon isotope discrimination calculations, there were no significant effects of clone or block on g_m. Across treatments, the mean g_m was 0.07 ± 0.04 mol m^{-2} s^{-1}.

Water use efficiency

Gas exchange

In June, there were no significant effects of clone or water treatment on WUE_i. In July, drought significantly reduced WUE_i (p=0.0016) from 46.1 ± 1.70 µmol CO_2 (mol $H_2O)^{-1}$ to 36.0 ± 5.84 µmol CO_2 (mol $H_2O)^{-1}$ in the moderate drought and 20.0 ± 5.78 µmol CO_2 (mol $H_2O)^{-1}$ in the severe drought treatment. In contrast, in November, drought significantly increased WUE_i (p=0.0046) from 62.34 ± 2.78 µmol CO_2 (mol $H_2O)^{-1}$ to 102.88 ± 13.35 µmol CO_2 (mol $H_2O)^{-1}$ in the moderate drought treatment. There were no differences among clones in any of the measurement dates.

Stable isotope discrimination

Needles collected for bulk $\delta^{13}C$ ($\delta^{13}C_{bl}$) before water treatments were initiated showed no significant differences between clones for $\delta^{13}C_{bl}$ (p=0.1322) with values of -31.6‰ ± 0.26 for clone I, -31.0‰ ± 0.56 for clone II, and -31.4‰ ± 0.53 for clone III.

$\delta^{13}C_{sc}$ varied between treatment averages of -31.8‰ and -26.6‰ across all treatments. A split-plot analysis of the soluble carbohydrates data across the two sampling dates showed a significant time by clone by water treatment interaction (p=0.0453). Further analysis was performed on each sampling date independently.

In the first sampling date, there was an interaction between clone and water treatment (p=0.0183; Figure 12). In the well-watered treatment, clone I had the highest

$\delta^{13}C_{sc}$, -30.1‰ ± 0.21 and clone III had the lowest, -31.8‰ ± 0.18. In the moderate drought treatment, clone II had the highest $\delta^{13}Cs_c$, -27.0‰ ± 0.30 and clone I had the lowest, -28.0‰ ± 0.43. The clones were not significantly different from one another in the severe drought treatment and averaged -27.0‰.

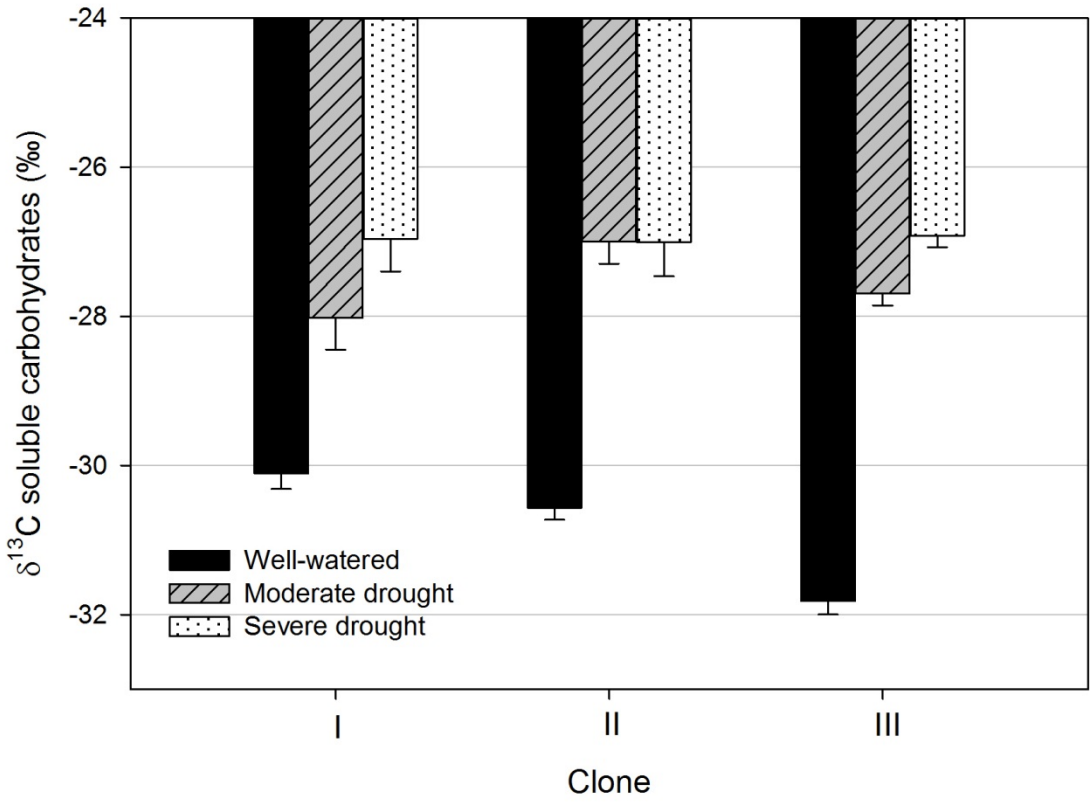

Figure 12. The $\delta^{13}C$ of soluble carbohydrates extracted from needles (n=4 for all clone by water treatments except for clone III in moderate drought, n=3) for June 27, 2013. There was a clone by water treatment interaction (p=0.0183).

In July, water treatment had a significant effect on $\delta^{13}C_{sc}$ ($p=0.0016$). The interactive effect between water treatment and clone was not significant at a 95% confidence level ($p=0.0980$). While the pattern of more negative $\delta^{13}C$ for well-watered treatments and less negative $\delta^{13}C$ for drought treatments was similar to the first measurement date for plants with Ψ_{PD} above -2.5 MPa, the plants exhibiting Ψ_{PD} below -2.5 MPa had lower $\delta^{13}C$, similar in value to the well-watered plants (Figure 13 and Figure 14). Here, the means of the treatments do not capture this response at low Ψ.

In the first measurement date, $\delta^{13}C_{sc}$ correlated better with g_s (Figure 15b; $R^2=0.57$, $p<.0001$) than with WUE_i (Figure 15a; $R^2=0.16$, $p=0.0163$). Stomatal conductance was less well correlated to $\delta^{13}C_{sc}$ in July (Figure 15d; $R^2=0.34$, $p=0.0003$), when the trees were under more severe drought stress and there was a decline in $\delta^{13}C_{sc}$ at very low Ψ.

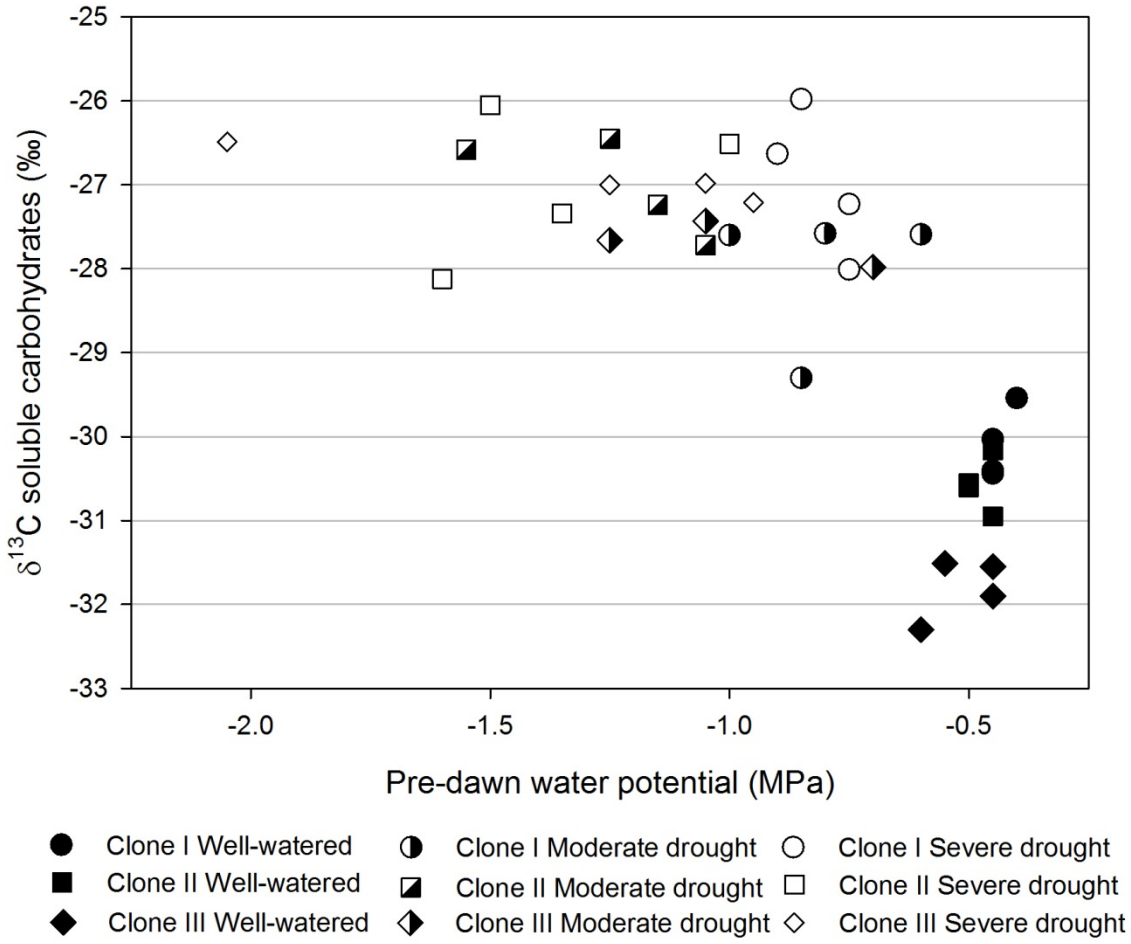

Figure 13. The 2013 $\delta^{13}C$ of soluble carbohydrates extracted from needles (n=4 for all clone by water treatments except for clone III in moderate drought, n=3) plotted against pre-dawn water potential for June 27, 2013.

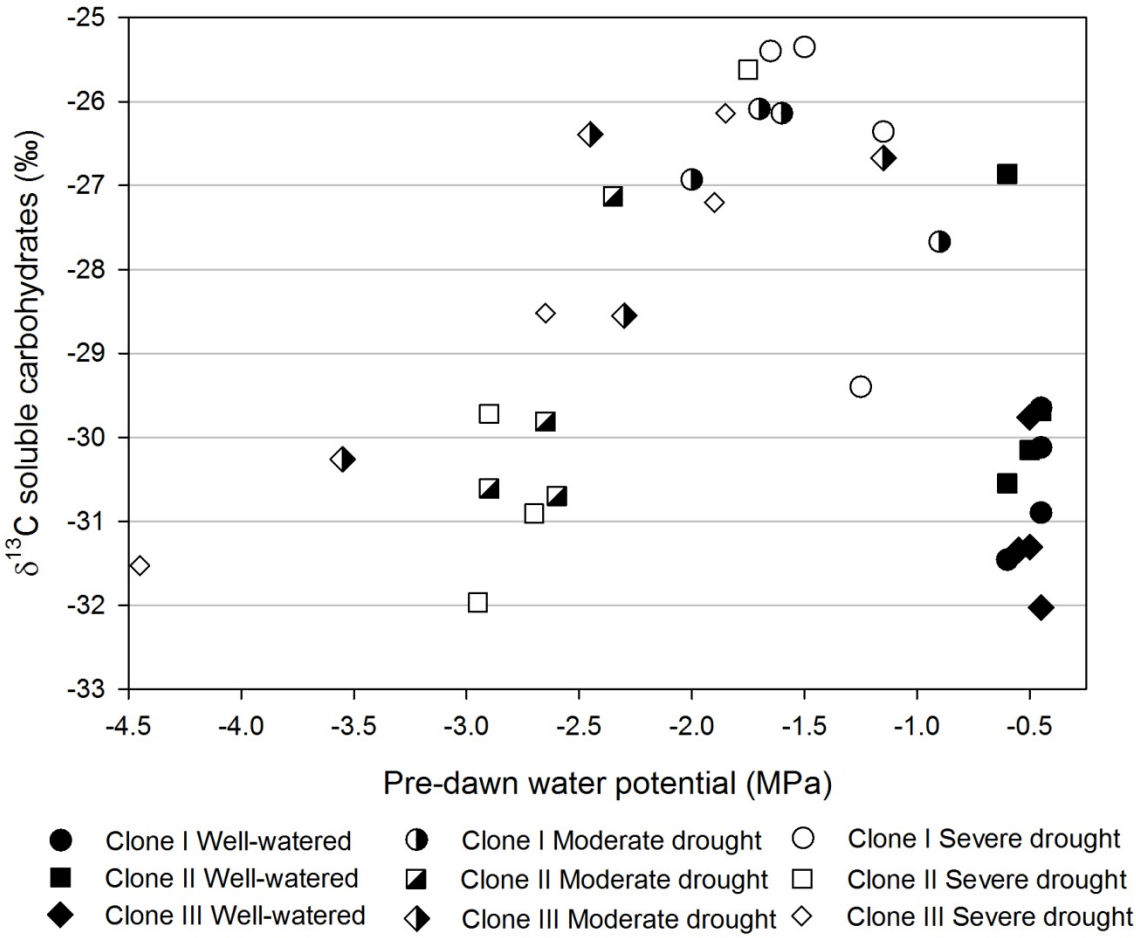

Figure 14. The $\delta^{13}C$ of soluble carbohydrates extracted from needles (n=4) plotted against pre-dawn water potential for July 23, 2013.

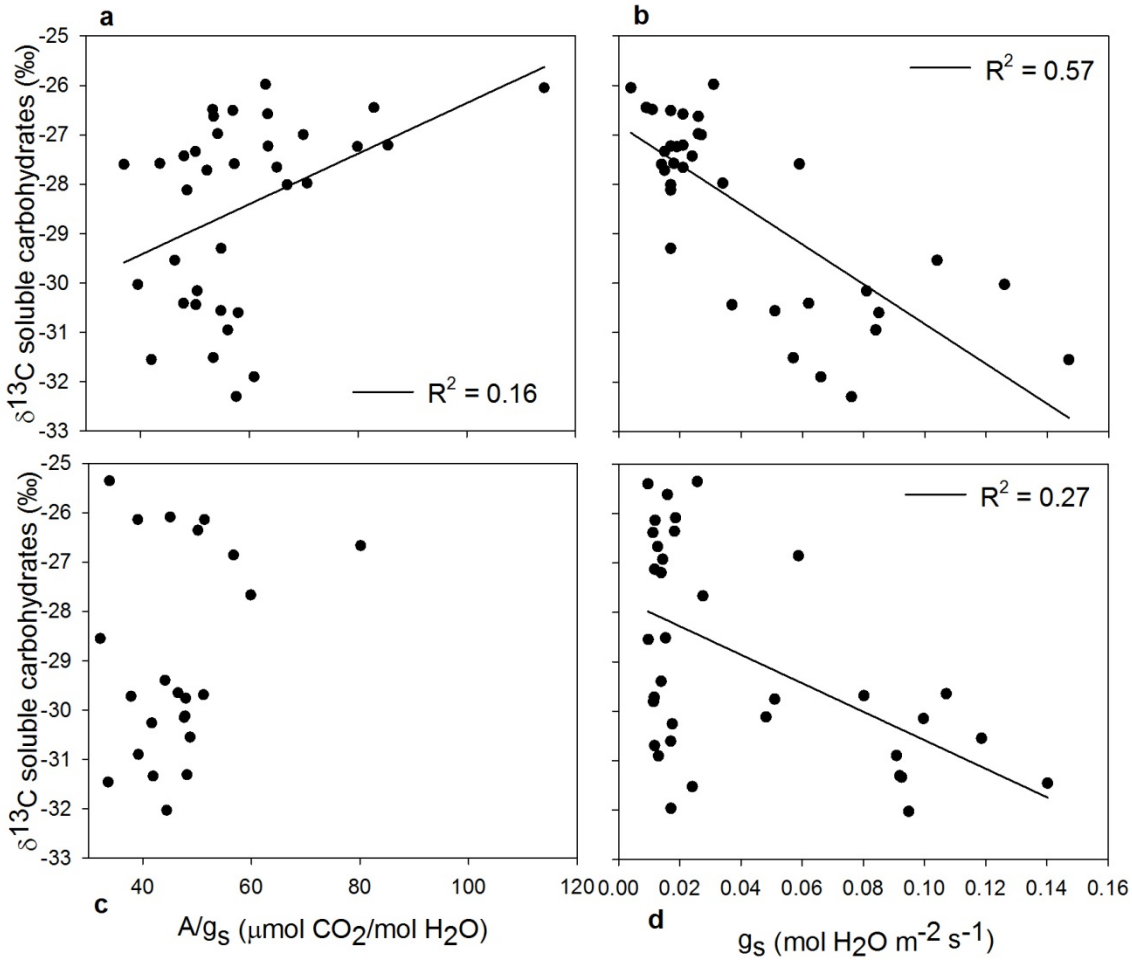

Figure 15. $\delta^{13}C$ of soluble carbohydrates by A/g_s and g_s for June (a and b) and July (c and d, trendlines significant at $p<0.05$).

The split-plot analysis showed that time did not have a significant effect on bulk leaf $\delta^{13}C$. The sampling dates were 26 days apart, so the relative contribution of new carbon to the isotopic composition of the bulk leaf carbon would be relatively small. There was, however, a significant clone effect ($p<.0001$) and clone by water treatment

interaction (p=0.021) when analyzed with the split-plot design. Across both dates, $\delta^{13}C_{bl}$ ranged from -31.5‰ ± 0.09 in clone III in the well-watered treatment to -29.8‰ ± 0.20 in clone I in the severe drought treatment (Figure 16).

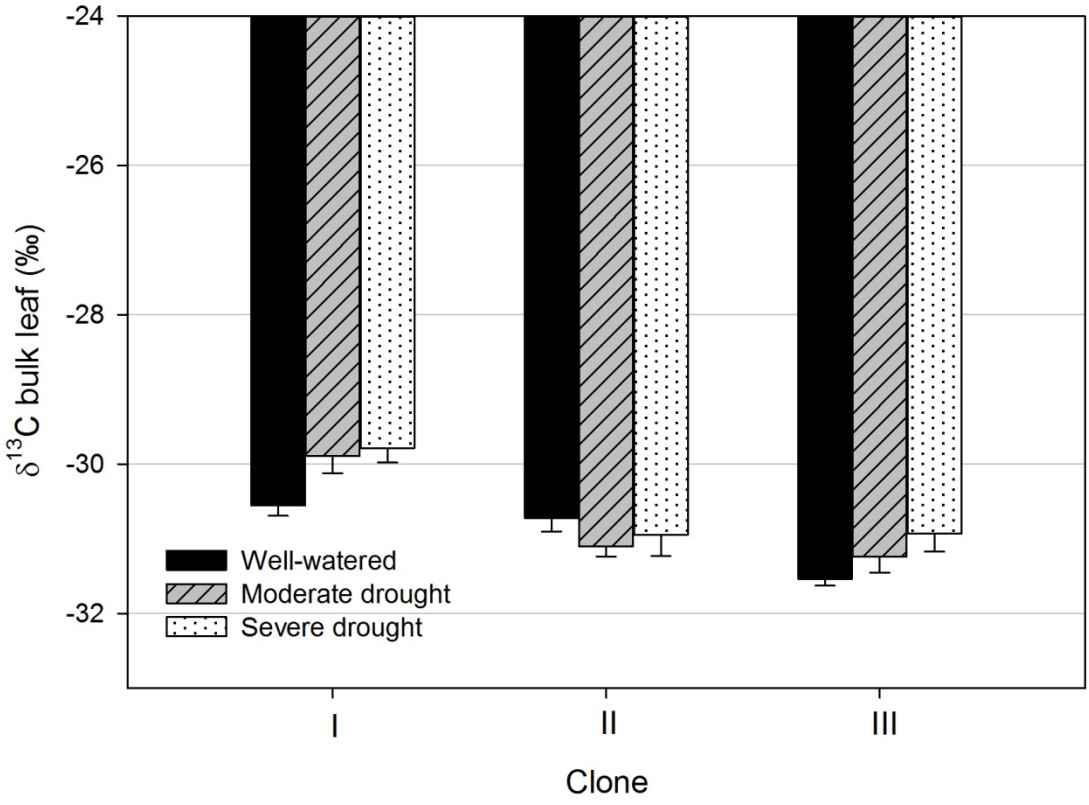

Figure 16. The average $\delta^{13}C$ of bulk leaf across dates for each treatment (n=4). There was a significant clone by water treatment interaction (p=0.021).

Hydraulic conductivity

Drought significantly decreased LSC ($p=0.0019$) by 42.6% (Figure 17a). Both clone ($p=0.0270$) and water treatment ($p=0.0043$) had significant effects on P_{50}, an indication of vulnerability to cavitation (Figure 17b). Drought decreased vulnerability to cavitation, with the P_{50} decreasing from -2.9 ± 0.16 MPa in the well-watered treatment to -3.9 ± 0.70 MPa in the moderate treatment, averaged across clones. Clone III was most vulnerable to cavitation, with a P_{50} of -3.0 ± 0.91 MPa, averaged across both treatments. Clone I was the least vulnerable to cavitation, with a P_{50} of -3.8 ± 0.27 MPa.

Growth

Growth rates

Significant three-way water treatment by clone by time interactions were observed for actual diameter ($p=0.0002$) and height ($p<.0001$) for May through November (Tables 2 and 3). Drought significantly reduced RGR ($p=0.0079$; Figure 18). Across treatments, RGR declined after July, so I evaluated the RGR for the period May to June to eliminate growth limitations in the well-watered treatment due to trees becoming pot-bound. Across clones and the period May to June, drought reduced RGR ($p=0.0079$) by 20.1%. RGR also varied by clone ($p<.0001$), with clone III the highest at 3.82 ± 0.246 g g^{-1} yr^{-1}, clone II at 3.49 ± 0.304 g g^{-1} yr^{-1}, and clone I the lowest at 1.54 ± 0.143 g g^{-1} yr^{-1}.

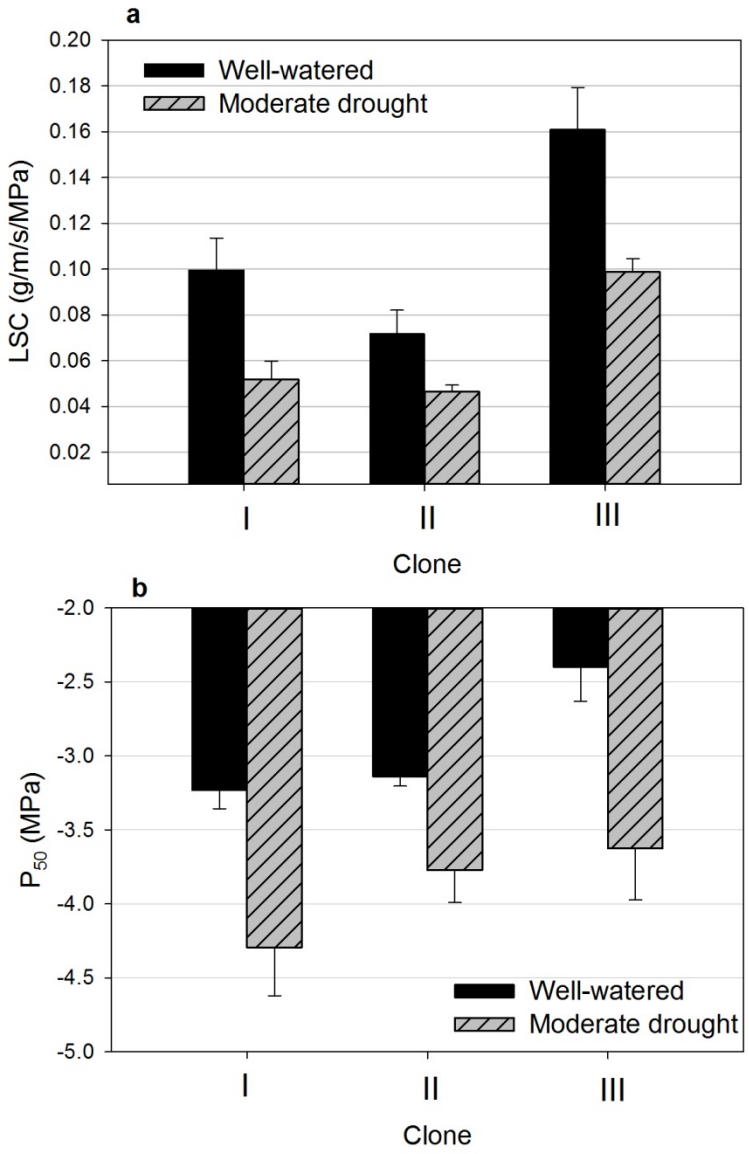

Figure 17. Leaf specific conductivity (a) and vulnerability to cavitation (b) (n=4 for all clone by water treatments except for clone II in well-watered treatment, n=3).

Table 2. ANOVA table for clone, water treatment, time, and their interactive effects on diameter

Effect	DF1	DF2	F-statistic	p-value
Clone	2	171	5.25	**0.0061**
Water treatment	1	171	10.85	**0.0012**
Clone x water treatment	2	171	5.10	**0.0070**
Time	3	171	18.11	**<.0001**
Time x clone	6	171	4.52	**0.0003**
Time x water treatment	3	171	13.84	**<.0001**
Clone x water treatment x time	6	171	4.66	**0.0002**

Table 3. ANOVA table for clone, water treatment, time, and their interactive effects on height

Effect	DF1	DF2	F-statistic	p-value
Clone	2	171	4.4	**0.0137**
Water treatment	1	171	3.14	0.0784
Clone x water treatment	2	171	8.2	**0.0004**
Time	3	171	35.5	**<.0001**
Time x clone	6	171	2.77	**0.0135**
Time x water treatment	3	171	6.85	**0.0002**
Clone x water treatment x time	6	171	5.02	**<.0001**

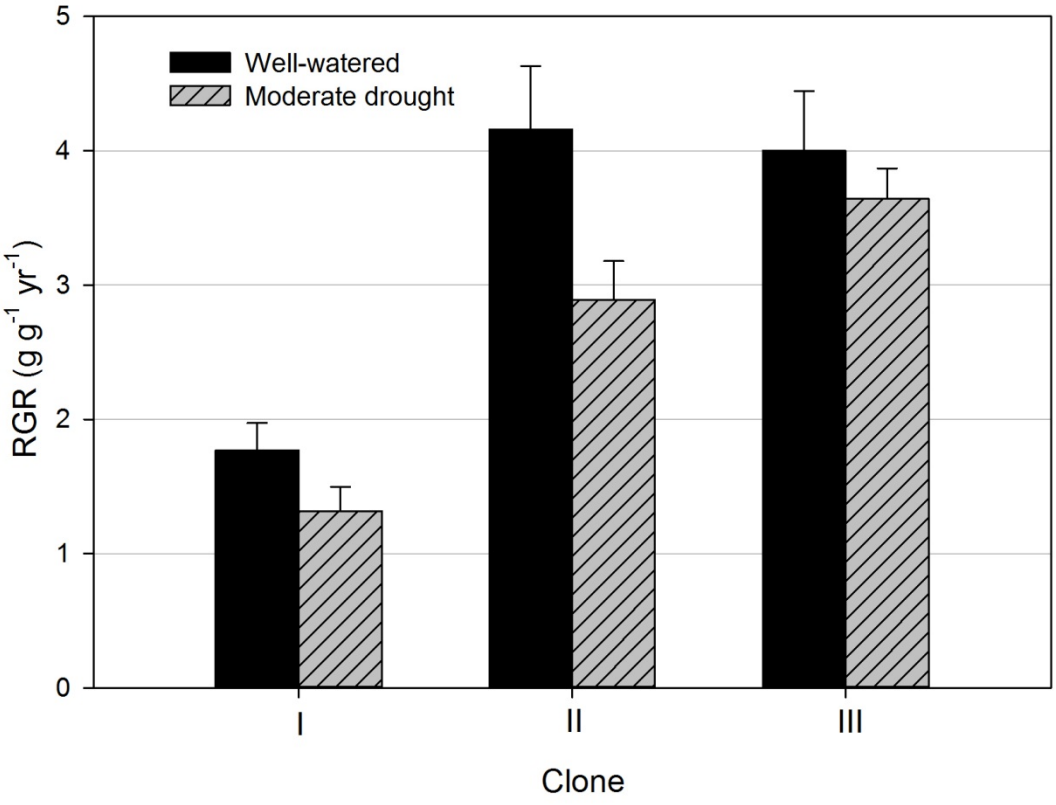

Figure 18. Relative growth rate from May to June (n=9 for all clone by water treatments except for clone II in well-watered treatment, n=3).

Diameter measurements

Diameter was a better predictor than height of overall biomass (Figure 19; R^2= 0.72 for diameter compared to R^2= 0.17 for height). Final diameter measurements were significantly different by clone (p=.0293) and water treatment (p<.0001) and had no interactive effect. Clone III had the largest final diameter at 9.11 ± 0.34 mm and clone I had the smallest diameter at 8.30 ± 0.32 mm averaged across treatments. Drought reduced the diameter by 22.2% overall.

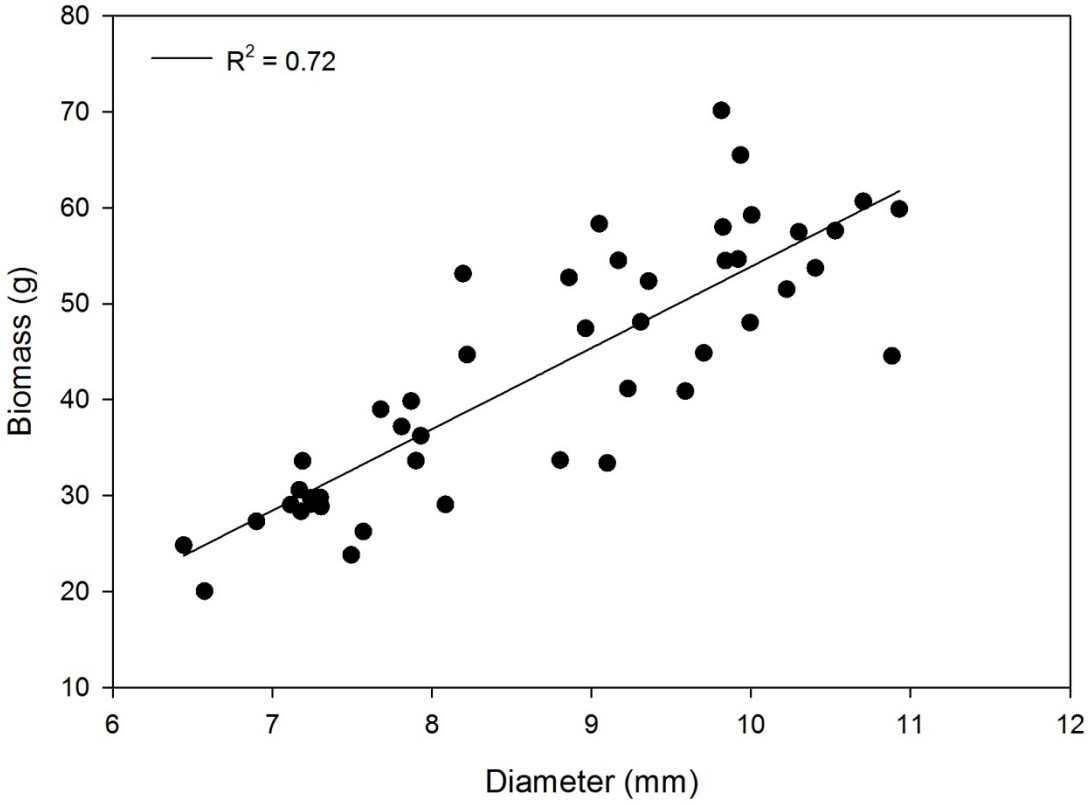

Figure 19. Linear fit for diameter and biomass across treatments ($p<0.05$).

Height measurements

There was an interactive effect of clone and water treatment on final height. Clone II for both well-watered and moderate drought treatments had the shortest heights, 66.13 ± 2.0061 cm and 58.88 ± 2.3838 cm, respectively. However, for the well-watered treatment, clone I was tallest at 84.17 ± 2.3746 cm, but for the moderate treatment, clone

III was tallest at 70.5714 ± 3.5881 cm. Drought reduced height by 22.6% in clone I, 11.0% in clone II, and 8.5% in clone III.

Biomass allocation

At harvest the main effects of clone and water treatment were significant for a number of biomass characteristics, and there were no clone by water treatment interactions (Table 4). There was a significant difference by clone for total needle dry mass ($p<.0001$), estimate of total needle area ($p<.0001$), root mass: leaf area ($p=0.0369$), and total biomass ($p=0.0033$; Figure 20), but not for root mass: leaf mass ratio ($p=0.3133$) or aboveground: belowground biomass ratio ($p=0.3508$). Clone II had the highest total needle mass, 41.2% higher than clone I and 53.8% higher than clone III. Clone II overall biomass was 28.0% higher than clone I and 25.7% higher than clone III. Clone I had the lowest overall root mass: leaf area ratio. Drought significantly decreased the total needle dry mass ($p<.0001$) by 41.7%, the estimate of leaf area ($p<.0001$), and total biomass ($p<.0001$) by 43.3% for all clones.

Table 4. ANOVA table for clone, water treatment, and clone x water treatment effects on leaf traits and biomass allocation.

Effect		**SLA**	**LMA**	**Total needle dry mass**	**Total needle area**	**Total biomass**	**Above: belowground biomass**	**Root mass: leaf area**
Clone	F-statistic	2.3611	2.0076	25.5243	17.4857	6.9044	1.0839	4.0883
	DF	2	2	2	2	2	2	2
	p-value	0.1111	0.1514	**<.0001**	**<.0001**	**0.0033**	0.3508	**0.0269**
Water treatment	F-statistic	0.6763	1.2897	137.2037	103.6218	151.7773	0.0998	0.0236
	DF	1	1	1	1	1	1	1
	p-value	0.4172	0.2648	**<.0001**	**<.0001**	**<.0001**	0.7542	0.8789
Clone x water treatment	F-statistic	0.5459	0.2170	2.1745	2.6002	0.2440	0.1482	0.5011
	DF	2	2	2	2	2	2	2
	p-value	0.5848	0.8061	0.1307	0.0909	0.7849	0.8628	0.6109

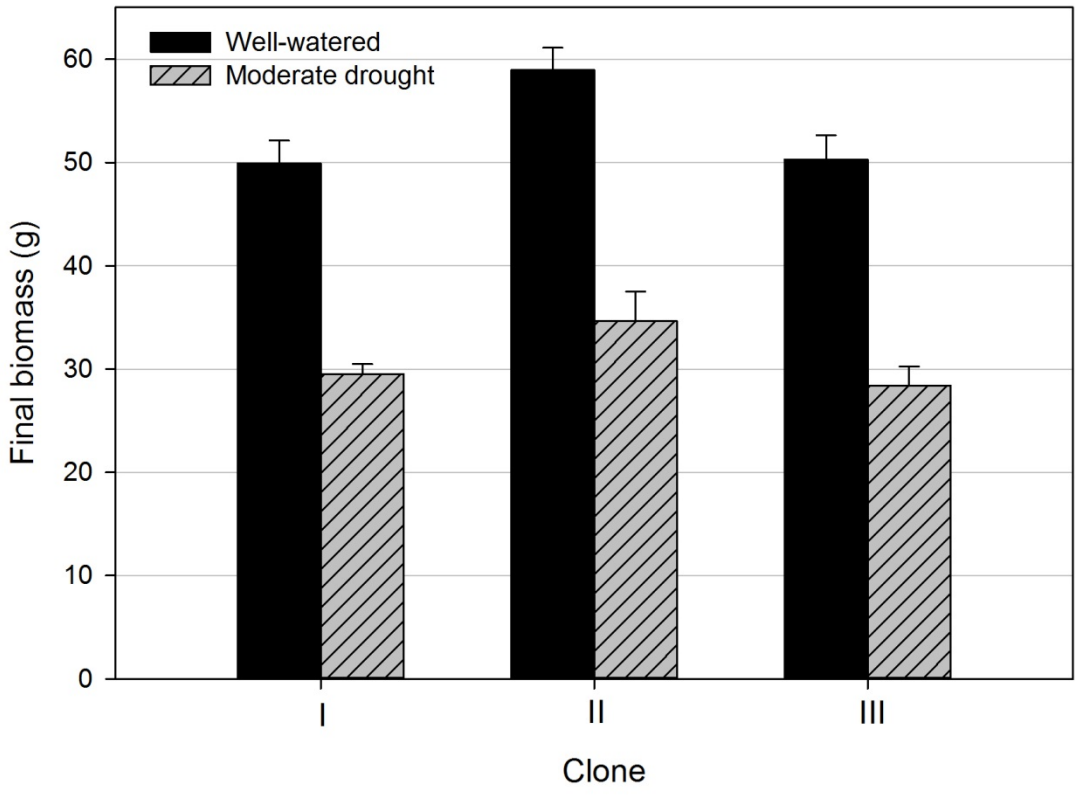

Figure 20. Final biomass (g) of well-watered treatment (black bars) of clone I (n=9), clone II (n=7), and clone III (n=9) and moderate drought treatment (dashed bars) of clone I (n=9), clone II (n=4), and clone III (n=7).

Discussion

A plant's adaptation to drought stress is expressed in a number of traits that fall along a spectrum in functional and structural plasticity. From the global patterns of leaf traits and growth strategies, I expected coordinated structural and physiological traits that affected productivity. I also expected mesophyll conductance to decrease under drought conditions, as has been shown in other species.

This study supports the importance of using clones in research by demonstrating genetic differences in response to drought even with clones that were not selected based on differences in traits. There is within-family variation of responses to environment and nutrient availability (King et al. 2008) but much of the research on loblolly pine does not use clones, so genetic variability cannot be examined. The three clones in this study do not represent the range of variation in the species but allowed a comparison of genetic versus phenotypic variation.

Coordination of traits

The first hypothesis, a coordination of leaf and structural traits, was partially supported. The clone with the highest RGR had the highest LSC and P_{50}. It displayed the lowest $\delta^{13}C_{sc}$ in well-watered conditions, but the clones had varying degrees of response in $\delta^{13}C_{sc}$ to drought. It has been reported that trees with high relative height growth rates have the highest vulnerability to cavitation in mature trees and trees than had lower relative height growth rates were less vulnerable (Domec and Gartner 2003). It was suggested that stomatal sensitivity was a plastic response that optimized carbon assimilation in conditions of high water availability and minimized water loss in low water availability. My findings were consistent with these patterns and provide evidence for genetic control over the degree of plasticity of stomatal conductance in response to drought.

Leaf physiology and gas exchange

Mesophyll conductance

My second hypothesis, that drought would decrease mesophyll conductance, was not supported by this study. Contrary to expectations, the statistical analysis of water treatment effect on g_m indicates that the clones in this study do not have a high plasticity of g_m in response to drought. If g_m does not vary significantly with drought in loblolly pine, the simplified Farquhar model should be adequate for describing carbon isotope discrimination based on g_s in this species.

I expected g_m of loblolly pine to decrease with water stress, as has been shown in other species at multiple time scales (Flexas et al. 2008). During the measurements of gas exchange and chlorophyll fluorescence, Ψ_{PD} for the moderate drought treatment were slightly lower than that of the well-watered treatment (-0.56 ± 0.02 MPa and -0.37 ±0.01 MPa, respectively) and A_n was not significantly different between treatments (at α=0.05). It is possible that g_m responds quickly to re-watering after drought and that the drought treatment was not experiencing low enough soil water availability. Mesophyll conductance has been shown to acclimate to water stress and recover from water stress (Flexas et al. 2009, Galle et al. 2009), so more frequent measurements may reveal changes over the course of drought and re-watering cycles. In my study, mesophyll conductance was measured after the trees had experienced several drought cycles, and if g_m acclimated to the drought, the timing of measurements could have missed the strongest influence of drought. However, this study does show that six months of drought conditions did not have an effect on g_m.

Because seasonality and light have been shown to affect g_m responses to water stress, others have concluded that environmental conditions affect this response (Flexas et al. 2009, Galle et al. 2009). Environmental factors other than soil moisture that might change the response of g_m such as light, temperature, and humidity were controlled in my study and a randomized complete block design minimized the effects of environmental gradients by location in the greenhouse.

Methods of estimating mesophyll conductance

Each method of estimating g_m has assumptions, estimated parameters, and data that contain error. There are many considerations for accuracy in gas exchange measurements, especially diffusion and leaks through the leaf chamber gasket. The curve fitting approach estimated four to five parameters simultaneously. Published curve-fitting methods may require specification of which region of the curve each point is associated with (Sharkey et al. 2007). The method used here, however, simultaneously estimated both limitations, RUBISCO and RUBP-regeneration, and the minimum of both curves was selected. This eliminated user-bias.

Chlorophyll fluorescence, as mentioned before, is sensitive to errors in Γ^*. Additionally, the leaf chamber for fluorescence measurements has an area of 2 cm^2, which can reduce the accuracy of measurements (Pons et al. 2009).

Estimates of g_m from $\delta^{13}C_{sc}$ are subject to errors based on limited integration of gas exchange measurements over a day (Pons et al. 2009). Following the methods of other studies that estimated g_m from $\delta^{13}C_{sc}$ (Scartazza et al. 1998, Monti et al. 2006, Centritto et al. 2009), the gas exchange measurements were made at single points in time

with saturating light conditions and were not representative of diurnal changes, whereas the soluble carbohydrates should integrate the past two or more days of A and g_s. Diurnal measurements of gas exchange at ambient conditions would be more accurate of the A and C_i that affect $\delta^{13}C_{sc}$, but even that temporal resolution is limited.

Finally, online carbon isotope discrimination and gas exchange measurements are subject to instrument precision and interference of one instrument on the other. Many fractionation and photosynthetic parameters are estimated for the equations used in this method. Farquhar and Cernusak (2012) assert that ternary effects of transpiration have not been included in g_m calculations from carbon isotopes, resulting in an overestimation of g_m. Also, high photosynthetic rates and leaf area should be used for a large difference between reference and sample CO_2, which maximizes the accuracy of isotopic discrimination (Pons et al. 2009).

The values for electron transport rate from chlorophyll fluorescence were much higher than values of J_{max} from the literature for loblolly pine (Wullschleger 1993, Aspinwall et al. 2011b). However, they are consistent with J_{max} standardized to 25°C in ambient CO_2 from data reported from the Duke FACE site, which ranged from 81 (±8) to 109 (±8) μmol m^{-2} s^{-1} (Ellsworth et al. 2012). Values of J_{max} and V_{cmax} from curve fitting are more consistent with other studies that used curve fitting, 20-30 μmol m^{-2} s^{-1} and 15-19 μmol m^{-2} s^{-1}, respectively (Wullschleger 1993).

Estimates of g_m are sensitive to errors in Γ* (Harley et al. 1992). The calculation of Γ* in this study, 28.87 μbar, was lower than that reported for other species, such as 38.7 μmol mol^{-1} for Eucalyptus, 43.08 μbar for tobacco, and approximately 40 μbar at

25°C for spinach and wheat (Brooks and Farquhar 1985, Harley et al. 1992, Douthe et al. 2011). The statistical analysis of significant effects does not change when using a value from the literature, such as 43.08 µbar. The value reported here of Γ* for loblolly pine supports the claim that Γ* may vary by species and should be measured.

Leaf mass per unit area

Along with g_m, the trees in this study did not have significant changes in leaf structure, LMA. The overall trend of LMA increase under drought stress is seen in other studies (Gu et al. 2012). Higher LMA is associated with lower photosynthetic capacity and leaf N% and a longer path length from the intercellular spaces to the chloroplast (Gu et al. 2012, Donovan et al. 2014). In addition, LMA in *P. taeda* has exhibited plastic responses to other environmental conditions such as quantum flux density (Niinemets et al. 2002). Needle density has also been seen to increase with needle age (Niinemets et al. 2002). From the evidence that needle morphology is plastic, it was surprising that the LMA did not significantly change with drought, even over six months of drought conditions.

Photosynthetic capacity

The correlation between A_n and foliar N concentration in my study was as strong as seen in other studies (Green and Mitchell 1992, King et al. 2008). Similar to Green and Mitchell (1992), the reduction in photosynthesis caused by drought was not affected by leaf N content. Also, in their study, N did not affect g_s in either well-watered or water stress conditions. The significance of this finding is that increasing fertilization neither improves nor reduces the water status of the plant.

Growth and productivity

In July, 86 days after drought treatments were implemented and 65 and 74 days without irrigation for the moderate and severe drought treatments, respectively, clone I had a significantly smaller diameter than the other clones while clone II was significantly shorter. However, by the end of the study, in November, there was not a significant difference in diameter for clone I and II. This suggests that clone I did not have as fast of growth in diameter as the other clones through the summer, but that it made up for that by faster growth than the other clones in the fall.

There are two possible explanations for these two clones tapering off in growth rate: they could have gotten pot bound or been affected by the period when the soil moisture in the well-watered treatment declined to 2%. At harvest, clone II had significantly higher belowground biomass than clones I and III, but clone III was not significantly different than clone I. The period of low water availability occurred in early July. At the June measurement date, clone I in the well-watered treatment had slightly higher, but not significantly different Ψ_{PD} and Ψ_{MD} than clones II and III. Instantaneous WUE from gas exchange data does not show that clone I is more WUE, but the $\delta^{13}C$ of soluble carbohydrates and bulk leaf at the end of June shows that clone I has significantly lower g_s than clone III, and is not significantly different than clone II. If clone I used less water than the other clones and dried down at a slower rate, it could explain why it was less affected by the longer period without irrigation.

Diameter was a better predictor of total biomass than height was (diameter R^2= 0.7159, height R^2= 0.1675) but the allometric equations used to estimate RGR include both diameter and height.

Because two clones in the well watered treatment exhibited reduced rates of growth at the end of the study, RGR was analyzed from the first part of the study after drought treatments were implemented. Based on other studies of loblolly pine, I would have expected the fastest growing and tallest trees to be the most WUE (Baltunis et al. 2008, Aspinwall et al. 2011b) because the most WUE trees would lose less water and maintain photosynthesis in drought conditions. The clones in this study do not appear to follow that trend. Instead, the fastest grower, clone III, had the lowest WUE in the well-watered treatment. This result supports the concept that yield and WUE are antithetical (Blum 2005) due to high productivity associated with high water use in non-water-limiting conditions.

The total needle dry mass at harvest indicates that clone II allocated more carbon to needles than to stem growth. In contrast, clones I and III allocated more carbon to stem growth (diameter and height) than to needle production. This pattern holds for both the well watered and drought treatments. In the well-watered treatment, clone II also had a higher root biomass and higher total biomass at harvest than the other clones. This type of growth would not be ideal for forest production in which you desire stem growth. However, clone II was more effective at biomass production. Loblolly pine families from Oklahoma/ Arkansas provenance were shown to accumulate more branch and foliage biomass than families from North Carolina Coastal provenances that have faster

height growth, even though the stem biomass accumulation and total aboveground biomass was not significantly different (Blazier et al. 2004). Clones vary in their allocation to root, stem, and foliage components (Tyree et al. 2009, Stovall et al. 2013). As loblolly trees develop, they allocate more biomass production to aboveground and less to belowground components (Albaugh et al. 2004).

While root area was not measured, root mass was used at the end of the experiment to analyze the clone and water treatment effects on root characteristics. Root: leaf area ratio describes the relative limitations from the soil and plant on water uptake (Sperry et al. 2002). Root: shoot ratio has been shown to be negatively correlated to mean annual precipitation (Mokany et al. 2006) and resource availability (Litton et al. 2007). I expected that the above: belowground biomass ratio would be affected by water stress because others had found that water stress decreased the root: shoot ratio of loblolly pine seedling biomass (Seiler and Johnson 1988). Water treatment did not have a significant effect on root: leaf mass ratio. Drought did significantly affect root mass: leaf area ratio, however, with clone III significantly higher than clone I in both treatments.

I expected drought to decrease biomass but also expected the ratio of above and belowground biomass to change. Allocation to root biomass or to fine roots would increase the plants' ability to access water in drought conditions. Under increased water availability, loblolly pine often reduces fine root production (Albaugh et al. 1998). Coarse and fine roots were not separated. Drought significantly decreased root biomass but did not affect the ratio of above: belowground biomass. At harvest, clone II had

significantly higher total and belowground biomass than clones I and III. This shows that clone II allocated more C to root growth and leaf area than to height and stem growth. This strategy maximizes water uptake from the soil and total photosynthetic capacity with the trade-off of slower height and diameter growth because of lower allocation to wood. Ewers et al. (2000) examined the interactions of fertilization and irrigation on loblolly pines and found that the decreased ability to extract water from the soil due to reduced root: leaf area ratio in fertilized trees was not as severe because the root xylem were also more resistant to cavitation under drought stress. Although the allocation did not change, I discuss the changes in hydraulic conductivity in the next section.

Hydraulic conductivity

Under well-watered conditions, the clone that had the lowest g_s exhibited the greatest LSC and the greatest vulnerability to cavitation. Drought reduced g_s, LSC, and the vulnerability to cavitation. It has been observed before that loblolly pine decreases hydraulic conductivity under low water conditions (Gonzalez-Benecke and Martin 2010). Sterck et al. (2008) stated that modeling studies typically predict an increase in LSC in response to drought, but they state that those studies have too many confounding factors from environmental conditions and genotypic and size differences. They reported a lower LSC at the dry site than the wet site and attributed this to a stronger effect of drought on conductance than leaf area. Similarly, my study found higher LSC in the well-watered treatment than the moderate drought treatment. Not only did drought decrease both conductivity and leaf area, it reduced the ability of the plant to transport water through the stem to each leaf. My study controlled genotype by the use of clones

and all plants were grown in a single greenhouse, with environmental gradients accounted for by blocking.

Loblolly pine exhibits phenotypic plasticity in water use traits in response to different soils and soil moisture conditions (Hacke et al. 2000). The whole tree hydraulic conductance and stomatal regulation of one loblolly pine plantation studied were coordinated in order to maintain a leaf Ψ as the soil dried (Domec et al. 2009). This coordination maintained values above Ψ_{PD} -0.8 MPa and Ψ_{MD} of -2.2 MPa, the limit where 80% loss of root hydraulic conductivity (Domec et al. 2009). The moderate and severe drought treatments in my experiment experienced similar water potentials in June (treatment averages ranging from -0.8 to -1.4 MPa for Ψ_{PD} and -1.3 to -1.7 MPa for Ψ_{MD}) and much lower Ψ during July (treatment averages ranging from -1.4 to -2.7 MPa for Ψ_{PD} of and -1.7 to –2.7 MPa for Ψ_{MD}). Drought decreased both hydraulic conductivity and stomatal conductance. Although $\delta^{13}C_{sc}$ was significantly correlated to g_s in June, there appears to be a threshold of Ψ_{PD} between the well-watered and drought treatments below which the $\delta^{13}C_{sc}$ shift to a higher value instead of a gradual shift. A study that examined plants at the point of slight water stress, within a narrow range of Ψ_{PD} that is regulated by g_s, may see a gradual change in $\delta^{13}C_{sc}$ that was not seen in my experiment.

Stem hydraulic properties and foliar $\delta^{13}C$ are connected by g_s and $\delta^{13}C$ should have an inverse relationship with LSC (Panek 1996). The relationship between LSC and $\delta^{13}C_{sc}$ in the current study trends in that direction but is not statistically significant.

$\delta^{13}C_{sc}$ was better correlated to g_s in June because there was an unexpected decline in $\delta^{13}C_{sc}$ at very low Ψ in July.

Regarding cavitation resistance, loblolly shows some genetic control, but there is also high plasticity (Hacke et al. 2000, Aspinwall et al. 2011a). The three clones in my study exhibited plasticity in P_{50} in response to drought. The well-watered trees displayed P_{50} values in the range reported by others for stem cavitation, -2.19 MPa to -3.50 MPa (Hacke et al. 2000, Aspinwall et al. 2011a), and the drought treatment averages were lower than this range. Clone III had the highest P_{50}, and this treatment also had the highest LSC, exhibiting the trade-off of high conductivity and high vulnerability to cavitation. An increase in LSC with increasing stem diameter has been reported, and this study has similar trends, with clone III having the largest diameter and LSC (Tyree et al. 1991). The plasticity in P_{50} response to drought was not significantly different by clone, but drought increased the P_{50} of clones I and III by a greater magnitude than that of clone II. Clone II had the lowest LSC and greatest root biomass. This clone's strategy of conservative LSC and high root mass for water uptake may relate to a low plasticity in resistance to cavitation whereas the clones with higher LSC and lower root mass must respond to drought to avoid catastrophic cavitation.

It is important to note that drought tolerance does not equal water use efficiency (Warren et al. 2001). Thus, the growth and survival of clones under drought stress depends as significantly on their ability to continue to conduct water as it does on their ability to assimilate carbon with lower g_s. I would expect the greater root production of clone II to make it better able to withstand drought. The focus of this study was water

use and drought responses, not drought tolerance versus avoidance strategies. Clone I, not clone II, had the lowest hydraulic conductivity and was the least vulnerable to cavitation. Drought decreased the hydraulic conductivity of the trees.

The prevailing concept of a trade-off between WUE and growth (Blum 2005) is not always accurate in pine species. One study found that the drought-hardy pine family of the Texas Lost Pines was slowest growing and also had the lowest WUE_i and $\delta^{13}C$ (Yang et al. 2002). They concluded that the families that they studied had different biomass allocations but not different leaf physiology. The Texas families, then, have strategies for avoiding drought, like deep root systems, small needles, and fewer stomata per leaf area, instead of being more WUE than the trees from areas with higher precipitation (Bilan et al. 1977, Yang et al. 2002). Further research on the plastic response of mesophyll conductance in loblolly pine could include these drought-tolerant genotypes.

Soluble carbohydrates isotopic composition

Carbon isotope ratios of plants are partially controlled by C_i/C_a, and are widely used as a proxy for stomatal conductance and water use efficiency (Farquhar et al. 1989). $\delta^{13}C$ integrates the plant's physiological response to environmental conditions over a period of time. Under well-watered conditions, $\delta^{13}C$ is an estimate of WUE. Under drought conditions, if the stomatal conductance supply of C decreases at a faster rate than the photosynthetic demand of C, then C_i and C discrimination will both decrease.

Carbon isotope composition of soluble carbohydrates

The isotopic composition of soluble carbohydrates was chosen for analysis instead of bulk leaf because $\delta^{13}C_{sc}$ integrates a shorter time period of photosynthesis and stomatal conductance. This is evidenced by the significant time effects on $\delta^{13}C_{sc}$ but not on $\delta^{13}C_{bl}$ across two sampling dates in which the trees experienced different levels of drought stress. Isolation of soluble carbohydrates is necessary for a representative sample of recent photosynthates because there is post-photosynthetic fractionation of carbon and varying turnover times for organic compounds, which causes a difference of isotopic composition of different plant parts and throughout the day. Thus, starches and sugars have different isotope values and the relative concentrations of these changes throughout a 24 hour period, causing a diurnal variation up to 1.9‰ in $\delta^{13}C$ of soluble organic matter (Brandes et al. 2006). For this reason, soluble carbohydrates were isolated and analyzed.

Correlation of carbon isotope composition and gas exchange

Neither soluble carbohydrates nor bulk leaf isotopic values significantly correlated to instantaneous measures of WUE. $\delta^{13}C_{bl}$ is not a good indicator of recent environmental conditions (Keitel et al. 2003). In one study on *Beta vulgaris* under drought, neither $\delta^{13}C_{bl}$ and $\delta^{13}C_{sc}$ correlated with net photosynthesis: transpiration ratio (A/E; instantaneous WUE), but did correlate with A/g_s (intrinsic WUE; Monti et al. 2006). My study found that $\delta^{13}C_{sc}$ had a better correlation with g_s than with A/g_s, which is likely due to the high sensitivity of g_s to drought. Drought reduced both A and g_s, which have counteracting effects on C_i, which in turn effects $\delta^{13}C_{sc}$. The better

correlation of $\delta^{13}C_{sc}$ and g_s than A/g_s indicated that g_s had greater influence than photosynthesis over C_i. This suggests that $\delta^{13}C_{sc}$ may be used as an indication of recent stomatal conductance, a correlation other studies have made (Keitel et al. 2003, Gessler et al. 2004, West et al. 2007). There was a significant drought and clone interactive effect on $\delta^{13}C_{sc}$. That interactive effect on WUE or g_s was not seen by measurements of gas exchange (A/g_s, or WUE_i).

There are other environmental factors that have been shown to affect $\delta^{13}C$ by their influence on photosynthesis, such as light and nutrient status (Warren et al. 2001). Others have reported that $\delta^{13}C$ was highly correlated to LMA but not with precipitation or water availability, which affect g_s (Vitousek et al. 1990). However, in my study, $\delta^{13}C$ of soluble carbohydrates was better correlated to g_s than to A or LMA.

The effect of drought on $\delta^{13}C_{sc}$ in June was expected, but the pattern in July was unusual. The plants were experiencing more severe water stress in July than in June, evidenced by lower Ψ_{PD}. One possible explanation for the pattern of isotope values under low water conditions in July is that the fraction of other neutral compounds remaining in the needles was substantial relative to carbohydrates, and if the delta value for these other compounds differs greatly from that of the bulk carbohydrates, this would affect the isotopic composition (Richter et al. 2009). On the other hand, Brandes et al. found that there were not differences between water-soluble carbon fraction and soluble carbohydrate fraction $\delta^{13}C$ (Brandes et al. 2006). They state that the amino acids and organic acids either had low concentrations or were similar in isotopic composition to the soluble carbohydrates. I cannot state definitively if this is the cause of the abnormal

pattern because I did not quantify the carbohydrate content or analyze the chemical composition of the extracted neutral compounds.

This interesting effect on $\delta^{13}C$ at Ψ_{PD} below -2.0 MPa has not been reported to my knowledge. I believe that the low photosynthesis for a long period of water stress caused the plant to mobilize reserves of carbon that would be isotopically different than carbohydrates of recent photosynthates. This low isotopic value of neutral compounds in the plant leaf could be one indication of "carbon starvation" or catastrophic cavitation that leads to mortality if the plant is no longer assimilating carbon but instead using carbon reserves for respiration. Starch is ^{13}C enriched compared to neutral fraction and bulk leaf (Göttlicher et al. 2006). Interestingly, clone I did not reach these low Ψ_{PD} and corresponding $\delta^{13}C$, possibly due to a more conservative water use strategy, evidenced by moderate LSC and $\delta^{13}C$ in well-watered conditions. Clone II had a steeper slope of decline in $\delta^{13}C$ below -2.0 MPa than clone III. This could indicate that clone II was less tolerant of drought and shut down photosynthesis earlier (at higher Ψ) than clone III. The phenomenon could be explored further in other studies to examine the mobilization of C reserves in plants that are closing stomata and reducing photosynthesis in response to drought.

Summary

In summary, there was genotypic variability in plasticity of WUE measured by $\delta^{13}C_{sc}$, but all clones responded the same to drought in other traits such as growth, photosynthesis, and stomatal conductance. Mesophyll conductance was not affected by

prolonged drought. Plant growth strategies by genotype were seen. The fastest growing clone had low WUE in well-watered conditions, high LSC and vulnerability to cavitation, and high stomatal sensitivity to drought. One clone exhibited a growth strategy of high allocation to roots and leaves and less to stem growth. This growth strategy was associated with moderate WUE, low LSC across treatments, and a less plastic response of LSC to drought. The clone that appeared to be the most drought-tolerant was the least vulnerable to cavitation and had the highest WUE in well-watered conditions. This clone appeared to acclimate to drought stress, but it had the lowest growth rate. From the growth strategies exhibited by the three clones in this study, planting the most drought-tolerant genotype will result in lower productivity.

SUMMARY

Although there were differences in plasticity of WUE by genotype and both genetics and drought significantly effected many structural and physiological traits, there was not conclusive evidence that g_m changed in response to drought. Loblolly pine is known to respond to drought in stomatal and hydraulic conductance, which this study confirmed. It may not be able to adjust mesophyll conductance.

Modifications should be made to the system described here that couples the LI-6400 gas exchange system to the CRDS laser. Different valves could be tested. Berryman et al.'s (2011) small volume manifold system could be adapted for this system in which the leaf chamber exhaust is collected in a flask and then injected into a line to the CRDS. This system of online carbon isotope and gas exchange analysis will allow us to estimate changes in g_m on short time scales.

REFERENCES

Albaugh, T. J., H. L. Allen, P. M. Dougherty, L. W. Kress, and J. S. King. 1998. Leaf area and above- and belowground growth responses of loblolly pine to nutrient and water additions. Forest Science **44**:317-328.

Albaugh, T. J., H. Lee Allen, P. M. Dougherty, and K. H. Johnsen. 2004. Long term growth responses of loblolly pine to optimal nutrient and water resource availability. Forest Ecology and Management **192**:3-19.

Allen, C. D., A. K. Macalady, H. Chenchouni, D. Bachelet, N. McDowell, M. Vennetier, T. Kitzberger, A. Rigling, D. D. Breshears, E. H. Hogg, P. Gonzalez, R. Fensham, Z. Zhang, J. Castro, N. Demidova, J.-H. Lim, G. Allard, S. W. Running, A. Semerci, and N. Cobb. 2010. A global overview of drought and heat-induced tree mortality reveals emerging climate change risks for forests. Forest Ecology and Management **259**:660-684.

Aspinwall, M. J., J. S. King, J.-C. Domec, S. E. McKeand, and F. Isik. 2011a. Genetic effects on transpiration, canopy conductance, stomatal sensitivity to vapour pressure deficit, and cavitation resistance in loblolly pine. Ecohydrology **4**:168-182.

Aspinwall, M. J., J. S. King, S. E. McKeand, and J.-C. Domec. 2011b. Leaf-level gas-exchange uniformity and photosynthetic capacity among loblolly pine (Pinus taeda L.) genotypes of contrasting inherent genetic variation. Tree Physiology **31**:78-91.

Baltunis, B., T. Martin, D. Huber, and J. Davis. 2008. Inheritance of foliar stable carbon isotope discrimination and third-year height in Pinus taeda clones on contrasting sites in Florida and Georgia. Tree Genetics & Genomes **4**:797-807.

Barbour, M. M., N. G. McDowell, G. Tcherkez, C. P. Bickford, and D. T. Hanson. 2007. A new measurement technique reveals rapid post-illumination changes in the carbon isotope composition of leaf-respired CO2. Plant, Cell & Environment **30**:469-482.

Barbour, M. M., C. R. Warren, G. D. Farquhar, G. Forrester, and H. Brown. 2010. Variability in mesophyll conductance between barley genotypes, and effects on transpiration efficiency and carbon isotope discrimination. Plant, Cell & Environment **33**:1176-1185.

Berryman, E. M., J. D. Marshall, T. Rahn, S. P. Cook, and M. Litvak. 2011. Adaptation of continuous-flow cavity ring-down spectroscopy for batch analysis of δ13C of CO2 and comparison with isotope ratio mass spectrometry. Rapid Communications In Mass Spectrometry **25**:2355-2360.

Bickford, C. P., N. G. McDowell, E. B. Erhardt, and D. T. Hanson. 2009. High-frequency field measurements of diurnal carbon isotope discrimination and internal conductance in a semi-arid species, Juniperus monosperma. Plant, Cell & Environment **32**:796-810.

Bilan, M. V., C. T. Hogan, and H. B. Carter. 1977. Stomatal opening, transpiration, and needle moisture in loblolly pine seedlings from two Texas seed sources. Forest Science **23**:457-462.

Blazier, M. A., T. C. Hennessey, T. B. Lynch, R. F. Wittwer, and M. E. Payton. 2004. Productivity, crown architecture, and gas exchange of North Carolina and Oklahoma/Arkansas loblolly pine families growing on a droughty site in southeastern Oklahoma. Forest Ecology and Management **194**:83-94.

Blum, A. 2005. Drought resistance, water-use efficiency, and yield potential—are they compatible, dissonant, or mutually exclusive? Australian Journal of Agricultural Research **56**:1159-1168.

Bowling, D. R., D. E. Pataki, and J. T. Randerson. 2008. Carbon isotopes in terrestrial ecosystem pools and CO2 fluxes. New Phytologist **178**:24-40.

Bowling, D. R., S. D. Sargent, B. D. Tanner, and J. R. Ehleringer. 2003. Tunable diode laser absorption spectroscopy for stable isotope studies of ecosystem–atmosphere CO2 exchange. Agricultural and Forest Meteorology **118**:1-19.

Brandes, E., N. Kodama, K. Whittaker, C. Weston, H. Rennenberg, C. Keitel, M. A. Adams, and A. Gessler. 2006. Short-term variation in the isotopic composition of organic matter allocated from the leaves to the stem of Pinus sylvestris: effects of photosynthetic and postphotosynthetic carbon isotope fractionation. Global Change Biology **12**:1922-1939.

Brodribb, T., T. J. Brodribb, and T. S. Feild. 2000. Stem hydraulic supply is linked to leaf photosynthetic capacity: evidence from New Caledonian and Tasmanian rainforests. Plant, Cell & Environment **23**:1381-1388.

Brooks, A. and G. D. Farquhar. 1985. Effect of temperature on the CO2/O2 specificity of ribulose-1,5-bisphosphate carboxylase/oxygenase and the rate of respiration in the light. Planta **165**:397-406.

Brugnoli, E., K. T. Hubick, S. v. Caemmerer, S. C. Wong, and G. D. Farquhar. 1988. Correlation between the carbon isotope discrimination in leaf starch and sugars of C3 plants and the ratio of intercellular and atmospheric partial pressures of carbon dioxide. Plant Physiology **88**:1418-1424.

Bunce, J. A. 2009. Use of the response of photosynthesis to oxygen to estimate mesophyll conductance to carbon dioxide in water-stressed soybean leaves. Plant, Cell & Environment **32**:875-881.

Centritto, M., M. Lauteri, M. C. Monteverdi, and R. Serraj. 2009. Leaf gas exchange, carbon isotope discrimination, and grain yield in contrasting rice genotypes subjected to water deficits during the reproductive stage. Journal of Experimental Botany **60**:2325-2339.

Cumbie, W. P., A. Eckert, J. Wegrzyn, R. Whetten, D. Neale, and B. Goldfarb. 2011. Association genetics of carbon isotope discrimination, height and foliar nitrogen in a natural population of Pinus taeda L. Heredity **107**:105-114.

Domec, J.-C., A. Noormets, J. S. King, G. Sun, S. G. McNulty, M. J. Gavazzi, J. L. Boggs, and E. A. Treasure. 2009. Decoupling the influence of leaf and root hydraulic conductances on stomatal conductance and its sensitivity to vapour pressure deficit as soil dries in a drained loblolly pine plantation. Plant, Cell & Environment **32**:980-991.

Domec, J.-C., J. Ogée, A. Noormets, J. Jouangy, M. Gavazzi, E. Treasure, G. Sun, S. G. McNulty, and J. S. King. 2012. Interactive effects of nocturnal transpiration and climate change on the root hydraulic redistribution and carbon and water budgets of southern United States pine plantations. Tree Physiology **32**:707-723.

Domec, J.-C., K. Schäfer, R. Oren, H. S. Kim, and H. R. McCarthy. 2010. Variable conductivity and embolism in roots and branches of four contrasting tree species and their impacts on whole-plant hydraulic performance under future atmospheric CO2 concentration. Tree Physiology **30**:1001-1015.

Domec, J. C. and B. L. Gartner. 2003. Relationship between growth rates and xylem hydraulic characteristics in young, mature and old-growth ponderosa pine trees. Plant, Cell & Environment **26**:471-483.

Donovan, L. A., C. M. Mason, A. W. Bowsher, E. W. Goolsby, and C. D. A. Ishibashi. 2014. Ecological and evolutionary lability of plant traits affecting carbon and nutrient cycling. Journal of Ecology **102**:302-314.

Douthe, C., E. Dreyer, D. Epron, and C. R. Warren. 2011. Mesophyll conductance to CO2, assessed from online TDL-AS records of 13CO2 discrimination, displays small but significant short-term responses to CO2 and irradiance in Eucalyptus seedlings. Journal of Experimental Botany **62**:5335-5346.

Ellsworth, D. S., R. Thomas, K. Y. Crous, S. Palmroth, E. Ward, C. Maier, E. DeLucia, and R. Oren. 2012. Elevated CO2 affects photosynthetic responses in canopy pine and subcanopy deciduous trees over 10 years: a synthesis from Duke FACE. Global Change Biology **18**:223-242.

Epron, D., D. Godard, G. Cornic, and B. Genty. 1995. Limitation of net CO2 assimilation rate by internal resistances to CO2 transfer in the leaves of two tree species (Fagus sylvatica L. and Castanea sativa Mill.). Plant, Cell & Environment **18**:43-51.

Evans, J. R., T. D. Sharkey, J. A. Berry, and G. D. Farquhar. 1986. Carbon isotope discrimination measured concurrently with gas exchange to investigate CO2 diffusion in leaves of higher plants. Functional Plant Biology **13**:281-292.

Evans, J. R. and S. Von Caemmerer. 2012. Temperature response of carbon isotope discrimination and mesophyll conductance in tobacco. Plant, Cell & Environment **36**: 745-756.

Ewers, B. E., R. Oren, and J. S. Sperry. 2000. Influence of nutrient versus water supply on hydraulic architecture and water balance in Pinus taeda. Plant, Cell & Environment **23**:1055-1066.

Farquhar, G. D., S. Caemmerer, and J. A. Berry. 1980. A biochemical model of photosynthetic CO2 assimilation in leaves of C3 species. Planta **149**:78-90.

Farquhar, G. D. and L. A. Cernusak. 2012. Ternary effects on the gas exchange of isotopologues of carbon dioxide. Plant, Cell & Environment **35**:1221-1231.

Farquhar, G. D., J. R. Ehleringer, and K. T. Hubick. 1989. Carbon isotope discrimination and photosynthesis. Annual Review of Plant Physiology and Plant Molecular Biology **40**:503-537.

Farquhar, G. D., M. H. O'Leary, and J. A. Berry. 1982. On the relationship between carbon isotope discrimination and the intercellular carbon dioxide concentration in leaves. Functional Plant Biology **9**:121-137.

Ferrio, J. P., M. Cuntz, C. Offermann, R. Siegwolf, M. Saurer, and A. Gessler. 2009. Effect of water availability on leaf water isotopic enrichment in beech seedlings shows limitations of current fractionation models. Plant, Cell & Environment **32**:1285-1296.

Flexas, J., M. Barón, J. Bota, J.-M. Ducruet, A. Gallé, J. Galmés, M. Jiménez, A. Pou, M. Ribas-Carbó, C. Sajnani, M. Tomàs, and H. Medrano. 2009. Photosynthesis limitations during water stress acclimation and recovery in the drought-adapted Vitis hybrid Richter-110 (V. berlandieri×V. rupestris). Journal of Experimental Botany **60**:2361-2377.

Flexas, J., M. Ribas-Carbó, A. Diaz-Espejo, J. Galmés, and H. Medrano. 2008. Mesophyll conductance to CO2: current knowledge and future prospects. Plant, Cell & Environment **31**:602-621.

Galle, A., I. Florez-Sarasa, M. Tomas, A. Pou, H. Medrano, M. Ribas-Carbo, and J. Flexas. 2009. The role of mesophyll conductance during water stress and recovery in tobacco (Nicotiana sylvestris): acclimation or limitation? Journal of Experimental Botany **60**:2379-2390.

Galmés, J., J. M. Ochogavía, J. Gago, E. J. Roldán, J. Cifre, and M. À. Conesa. 2013. Leaf responses to drought stress in Mediterranean accessions of Solanum

lycopersicum: anatomical adaptations in relation to gas exchange parameters. Plant, Cell & Environment **36**:920-935.

Gessler, A., H. Rennenberg, and C. Keitel. 2004. Stable isotope composition of organic compounds transported in the phloem of European beech - evaluation of different methods of phloem sap collection and assessment of gradients in carbon isotope composition during leaf-to-stem transport. Plant Biology **6**:721-729.

Ginn, S. E., J. R. Seiler, B. H. Cazell, and R. E. Kreh. 1991. Physiological and growth responses of eight-year-old loblolly pine stands to thinning. Forest Science **37**:1030-1040.

Gonzalez-Benecke, C. A. and T. A. Martin. 2010. Water availability and genetic effects on water relations of loblolly pine (Pinus taeda) stands. Tree Physiology **30**:376-392.

González-Martínez, S. C., D. Huber, E. Ersoz, J. M. Davis, and D. B. Neale. 2008. Association genetics in Pinus taeda L. II. Carbon isotope discrimination. Heredity **101**:19-26.

Göttlicher, S., A. Knohl, W. Wanek, N. Buchmann, and A. Richter. 2006. Short-term changes in carbon isotope composition of soluble carbohydrates and starch: from canopy leaves to the root system. Rapid Communications In Mass Spectrometry **20**:653-660.

Green, T. H. and R. J. Mitchell. 1992. Effects of nitrogen on the response of loblolly pine to water stress. I. Photosynthesis and stomatal conductance. New Phytologist **122**:627-633.

Gu, J., X. Yin, T.-J. Stomph, H. Wang, and P. C. Struik. 2012. Physiological basis of genetic variation in leaf photosynthesis among rice (Oryza sativa L.) introgression lines under drought and well-watered conditions. Journal of Experimental Botany **63**:5137-5153.

Hacke, U. G., J. S. Sperry, B. E. Ewers, D. S. Ellsworth, K. V. R. Schäfer, and R. Oren. 2000. Influence of soil porosity on water use in Pinus taeda. Oecologia **124**:495-505.

Hacke, U. G., J. S. Sperry, J. K. Wheeler, and L. Castro. 2006. Scaling of angiosperm xylem structure with safety and efficiency. Tree Physiology **26**:689-701.

Harley, P. C., F. Loreto, G. D. Marco, and T. D. Sharkey. 1992. Theoretical considerations when estimating the mesophyll conductance to CO2 flux by analysis of the response of photosynthesis to CO2. Plant Physiology **98**:1429-1436.

Hobbie, E. A. and R. A. Werner. 2004. Tansley review. Intramolecular, compound-specific, and bulk carbon isotope patterns in C3 and C4 plants: a review and synthesis. New Phytologist **161**:371-385.

Jones, H. G. 1992. Plants and microclimate : a quantitative approach to environmental plant physiology. Cambridge University Press, Cambridge, United Kingdom and New York, NY, USA.

Keitel, C., M. A. Adams, T. Holst, A. Matzarakis, H. Mayer, H. Rennenberg, and A. Geßler. 2003. Carbon and oxygen isotope composition of organic compounds in

the phloem sap provides a short-term measure for stomatal conductance of European beech (Fagus sylvatica L.). Plant, Cell & Environment **26**:1157-1168.

King, N. T., J. R. Seiler, T. R. Fox, and K. H. Johnsen. 2008. Post-fertilization physiology and growth performance of loblolly pine clones. Tree Physiology **28**:703-711.

Kozlowski, T. T. and S. G. Pallardy. 2002. Acclimation and adaptive responses of woody plants to environmental stresses. The Botanical Review **68**:270-334.

Kramer, P. J. 1983. Water relations of plants. Academic Press, New York, New York.

Litton, C. M., J. W. Raich, and M. G. Ryan. 2007. Carbon allocation in forest ecosystems. Global Change Biology **13**:2089-2109.

Lloyd, J., J. P. Syvertsen, P. E. Kriedemann, and G. D. Farquhar. 1992. Low conductances for CO2 diffusion from stomata to the sites of carboxylation in leaves of woody species. Plant, Cell & Environment **15**:873-899.

Loreto, F., P. C. Harley, G. D. Marco, and T. D. Sharkey. 1992. Estimation of mesophyll conductance to CO2 flux by three different methods. Plant Physiology **98**:1437-1443.

Manter, D. K. and J. Kerrigan. 2004. A/Ci curve analysis across a range of woody plant species: influence of regression analysis parameters and mesophyll conductance. Journal of Experimental Botany **55**:2581-2588.

Marshall, J. D., J. R. Brooks, and K. Lajtha. 2008. Sources of variation in the stable isotopic composition of plants. R. Michener and K. Lajtha, editors. Pages 22-60

in Stable Isotopes in Ecology and Environmental Science. Blackwell Publishing Ltd.

Mokany, K., R. J. Raison, and A. S. Prokushkin. 2006. Critical analysis of root : shoot ratios in terrestrial biomes. Global Change Biology **12**:84-96.

Monti, A., E. Brugnoli, A. Scartazza, and M. T. Amaducci. 2006. The effect of transient and continuous drought on yield, photosynthesis and carbon isotope discrimination in sugar beet (Beta vulgaris L.). Journal of Experimental Botany **57**:1253-1262.

Niinemets, Ü., D. S. Ellsworth, A. Lukjanova, and M. Tobias. 2002. Dependence of needle architecture and chemical composition on canopy light availability in three North American Pinus species with contrasting needle length. Tree Physiology **22**:747-761.

Panek, J. A. 1996. Correlations between stable carbon-isotope abundance and hydraulic conductivity in Douglas-fir across a climate gradient in Oregon, USA. Tree Physiology **16**:747-755.

Peguero-Pina, J. J., J. Flexas, J. Galmés, Ü. Niinemets, D. Sancho-Knapik, G. Barredo, D. Villarroya, and E. Gil-Pelegrín. 2012. Leaf anatomical properties in relation to differences in mesophyll conductance to CO2 and photosynthesis in two related Mediterranean Abies species. Plant, Cell & Environment **35**:2121-2129.

Pittermann, J., J. S. Sperry, J. K. Wheeler, U. G. Hacke, and E. H. Sikkema. 2006. Mechanical reinforcement of tracheids compromises the hydraulic efficiency of conifer xylem. Plant, Cell & Environment **29**:1618-1628.

Pons, T. L., J. Flexas, S. v. Caemmerer, J. R. Evans, B. Genty, M. Ribas-Carbo, and E. Brugnoli. 2009. Estimating mesophyll conductance to CO2: methodology, potential errors, and recommendations. Journal of Experimental Botany **60**:2217-2234.

Poorter, H. and O. Nagel. 2000. The role of biomass allocation in the growth response of plants to different levels of light, CO2, nutrients and water: a quantitative review. Functional Plant Biology **27**:595-607.

Rella, C. Accurate stable carbon isotope ratio measurements with rapidly varying carbon dioxide concentrations using the Picarro d13CO2 G2101-i gas analyzer. Picarro, Inc., Sunnyvale, California.

Richter, A., W. Wanek, R. A. Werner, J. Ghashghaie, M. Jäggi, A. Gessler, E. Brugnoli, E. Hettmann, S. G. Göttlicher, Y. Salmon, C. Bathellier, N. Kodama, S. Nogués, A. Søe, F. Volders, K. Sörgel, A. Blöchl, R. T. W. Siegwolf, N. Buchmann, and G. Gleixner. 2009. Preparation of starch and soluble sugars of plant material for the analysis of carbon isotope composition: a comparison of methods. Rapid Communications In Mass Spectrometry **23**:2476-2488.

Scartazza, A., M. Lauteri, M. C. Guido, and E. Brugnoli. 1998. Carbon isotope discrimination in leaf and stem sugars, water-use efficiency and mesophyll conductance during different developmental stages in rice subjected to drought. Functional Plant Biology **25**:489-498.

Seibt, U., A. Rajabi, H. Griffiths, and J. A. Berry. 2008. Carbon isotopes and water use efficiency: sense and sensitivity. Oecologia **155**:441-454.

Seiler, J. R. and J. D. Johnson. 1988. Physiological and morphological responses of three half-sib families of loblolly pine to water-stress conditioning. Forest Science **34**:487-495.

Sharkey, T. D. 2012. Mesophyll conductance: constraint on carbon acquisition by C3 plants. Plant, Cell & Environment **35**:1881-1883.

Sharkey, T. D., C. J. Bernacchi, G. D. Farquhar, and E. L. Singsaas. 2007. Fitting photosynthetic carbon dioxide response curves for C3 leaves. Plant, Cell & Environment **30**:1035-1040.

Sperry, J. S. 2000. Hydraulic constraints on plant gas exchange. Agricultural and Forest Meteorology **104**:13-23.

Sperry, J. S., U. G. Hacke, R. Oren, and J. P. Comstock. 2002. Water deficits and hydraulic limits to leaf water supply. Plant, Cell & Environment **25**:251-263.

Sperry, J. S., U. G. Hacke, and J. Pittermann. 2006. Size and function in conifer tracheids and angiosperm vessels. American Journal of Botany **93**:1490-1500.

Sperry, J. S. and N. Z. Saliendra. 1994. Intra- and inter-plant variation in xylem cavitation in Betula occidentalis. Plant, Cell & Environment **17**:1233-1241.

Sterck, F. J., R. Zweifel, U. Sass-Klaassen, and Q. Chowdhury. 2008. Persisting soil drought reduces leaf specific conductivity in Scots pine (Pinus sylvestris) and pubescent oak (Quercus pubescens). Tree Physiology **28**:529-536.

Stocker, T. F., D. Qin, G.-K. Plattner, M. Tignor, S.K. Allen, J. Boschung, A. Nauels, Y. Xia, V. Bex and P.M. Midgley, editor. 2013. Climate change 2013: the physical science basis. Contribution of working group I to the fifth assessment report of

the Intergovernmental Panel on Climate Change. Cambridge University Press, Cambridge, United Kingdom and New York, NY, USA.

Stovall, J. P., T. R. Fox, and J. R. Seiler. 2013. Allometry varies among 6-year-old Pinus taeda (L.) clones in the Virginia Piedmont. Forest Science **59**:50-62.

Sultan, S. E. 2000. Phenotypic plasticity for plant development, function and life history. Trends in Plant Science **5**:537-542.

Tazoe, Y., S. Von Caemmerer, G. M. Estavillo, and J. R. Evans. 2011. Using tunable diode laser spectroscopy to measure carbon isotope discrimination and mesophyll conductance to CO_2 diffusion dynamically at different CO_2 concentrations. Plant, Cell & Environment **34**:580-591.

Tholen, D., C. Boom, and X.-G. Zhu. 2012. Opinion: Prospects for improving photosynthesis by altering leaf anatomy. Plant Science **197**:92-101.

Tjoelker, M. G., J. M. Craine, D. Wedin, P. B. Reich, and D. Tilman. 2005. Linking leaf and root trait syndromes among 39 grassland and savannah species. The New Phytologist **167**:493-508.

Tosens, T., Ü. Niinemets, V. Vislap, H. Eichelmann, and P. Castro Díez. 2012. Developmental changes in mesophyll diffusion conductance and photosynthetic capacity under different light and water availabilities in Populus tremula: how structure constrains function. Plant, Cell & Environment **35**:839-856.

Tyree, M. C., J. R. Seiler, and C. A. Maier. 2009. Short-term impacts of nutrient manipulations on leaf gas exchange and biomass partitioning in contrasting 2-

year-old Pinus taeda clones during seedling establishment. Forest Ecology and Management **257**:1847-1858.

Tyree, M. T. and F. W. Ewers. 1991. Tansley review No. 34. The hydraulic architecture of trees and other woody plants. New Phytologist **119**:345-360.

Tyree, M. T., D. A. Snyderman, T. R. Wilmot, and J.-L. Machado. 1991. Water relations and hydraulic architecture of a tropical tree (Schefflera morototoni) data, models, and a comparison with two temperate species (Acer saccharum and Thuja occidentalis). Plant Physiology **96**:1105-1113.

U.S. Environmental Protection Agency, C. C. D. 2013. Inventory of U.S. greenhouse gas emissions and sinks: 1990-2011. Reports & Assessments, Washington, DC.

Vitousek, P. M., C. B. Field, and P. A. Matson. 1990. Variation in foliar δ 13C in Hawaiian Metrosideros polymorpha: a case of internal resistance? Oecologia **84**:362-370.

von Caemmerer, S., J. R. Evans, G. S. Hudson, and T. J. Andrews. 1994. The kinetics of ribulose-1,5-bisphosphate carboxylase/oxygenase in vivo inferred from measurements of photosynthesis in leaves of transgenic tobacco. Planta **195**:88-97.

von Caemmerer, S. and R. Evans. 1991. Determination of the average partial pressure of CO2 in chloroplasts from leaves of several C3 plants. Australian Journal of Plant Physiology **18**:287-305.

Warren, C., J. McGrath, and M. Adams. 2001. Water availability and carbon isotope discrimination in conifers. Oecologia **127**:476-486.

Warren, C. R. 2005. Why does photosynthesis decrease with needle age in Pinus pinaster? Trees **20**:157-164.

Warren, C. R. and M. A. Adams. 2006. Internal conductance does not scale with photosynthetic capacity: implications for carbon isotope discrimination and the economics of water and nitrogen use in photosynthesis. Plant, Cell & Environment **29**:192-201.

Wertin, T. M., M. A. McGuire, and R. O. Teskey. 2012. Effects of predicted future and current atmospheric temperature and [CO2] and high and low soil moisture on gas exchange and growth of Pinus taeda seedlings at cool and warm sites in the species range. Tree Physiology **32**:847-858.

West, A. G., K. R. Hultine, K. G. Burtch, and J. R. Ehleringer. 2007. Seasonal variations in moisture use in a piñon–juniper woodland. Oecologia **153**:787-798.

Woelk, M. Simple, real-time measurement of stable isotope ratios in H2O and CO2. Picarro, Inc., Sunnyvale, CA.

Wright, I. J., P. B. Reich, M. Westoby, D. D. Ackerly, Z. Baruch, F. Bongers, J. Cavender-Bares, T. Chapin, J. H. C. Cornelissen, M. Diemer, J. Flexas, E. Garnier, P. K. Groom, J. Gulias, K. Hikosaka, B. B. Lamont, T. Lee, W. Lee, C. Lusk, J. J. Midgley, M.-L. Navas, Ü. Niinemets, J. Oleksyn, N. Osada, H. Poorter, P. Poot, L. Prior, V. I. Pyankov, C. Roumet, S. C. Thomas, M. G. Tjoelker, E. J. Veneklaas, and R. Villar. 2004. The worldwide leaf economics spectrum. Nature **428**:821-827.

Wullschleger. 1993. Biochemical limitations to carbon assimilation in C3 plants -- a retrospective analysis of the A/Ci curves from 109 species. Journal of Experimental Botany **44**:907-920.

Yang, W. Q., R. Murthy, P. King, and M. A. Topa. 2002. Diurnal changes in gas exchange and carbon partitioning in needles of fast- and slow-growing families of loblolly pine (Pinus taeda). Tree Physiology **22**:489-498.

Zhao, M. and S. W. Running. 2010. Drought-induced reduction in global terrestrial net primary production from 2000 through 2009. Science **329**:940-943.

APPENDIX

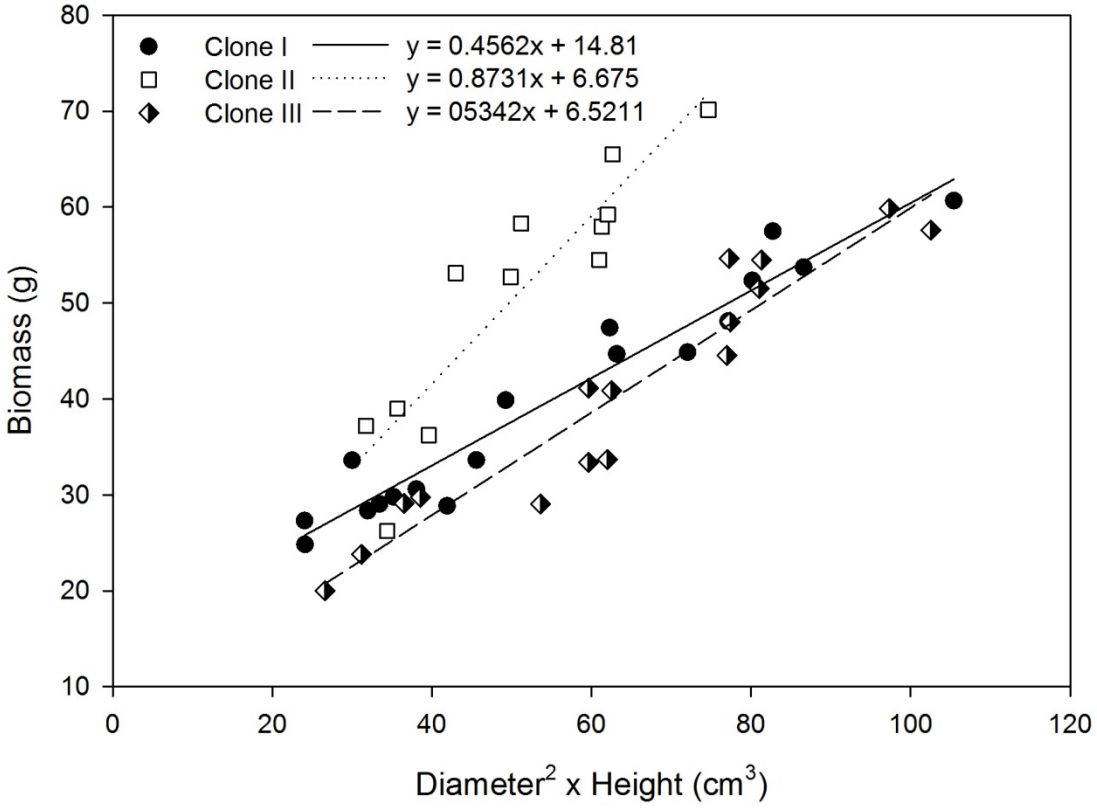

Figure A-1. Linear regressions for final biomass and diameter squared times height for clone I (n=18; R^2=0.94), clone II (n=12; R^2=0.83), and clone III (n=16; R^2=0.91).